

Reactor Physics Research at Purdue for the US NRC

T.J. Downar
Professor
Purdue University



Research Group

Yunlin Xu, Post-Doc

Deok Jung Lee, Post-Doc

Tomas Kozlowski, PhD Student

Zhaopeng Zhong, PhD Student

Justin Thomas, PhD Student

Jun Gan, PhD Student

Volkan Seker, PhD Student

Chris Cotton, MS Student

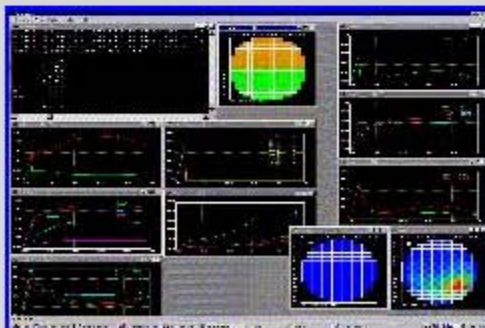


Purdue Advanced Reactor Core Simulator

Purdue University > Purdue Advanced Reactor Core Simulator >

PARCS: Computer Code

- Manual
 - [Theory](#)
 - [Users](#)
 - [Programmers](#)
 - [Software Quality Assurance](#)
- [Test Suite](#)
- [New Functionality](#)
 - [New Cross Section Model](#)
 - [Depletion Code System](#)
 - [Hexagonal Solution Model](#)
- [Support](#)



PARCS: Research Group



- [Downar, Thomas J.](#)
- [Gan, Jun](#)
- [Kozlowski, Tomasz](#)
- [Lee, Deokjung](#)
- [Lee, Hyun Chul](#)
- [Miller, R. Matt](#)
- [Thomas, Justin](#)
- [Xu, Yunlin](#)
- [Zhaopeng, Zhong](#)
- [Alumni](#)

Research Group Focus

- U.S. NRC
 - Reactor Physics Methods Development (PBMR, LWR MOX, ACR)
 - Coupled Neutronics/Thermal-Hydraulic Code Development for Reactor Transient Simulation
- U.S. DOE
 - Reactor Design and Fuel Cycle for Advanced Reactor Concepts (NERI: 2000-2004)
 - Coupled CFD/MOC (INERI)
 - Numerical Methods (NEER)
- Homeland Security

PARCS: Purdue Advanced Reactor Core Simulator

**A Multidimensional Multigroup Reactor
Kinetics Code Based on the Nonlinear
Nodal Method**



Prepared for Release of PARCS / NRC-V2.5

**Thomas J. Downar
Han Gyu Joo
Douglas A. Barber
Matt Miller**

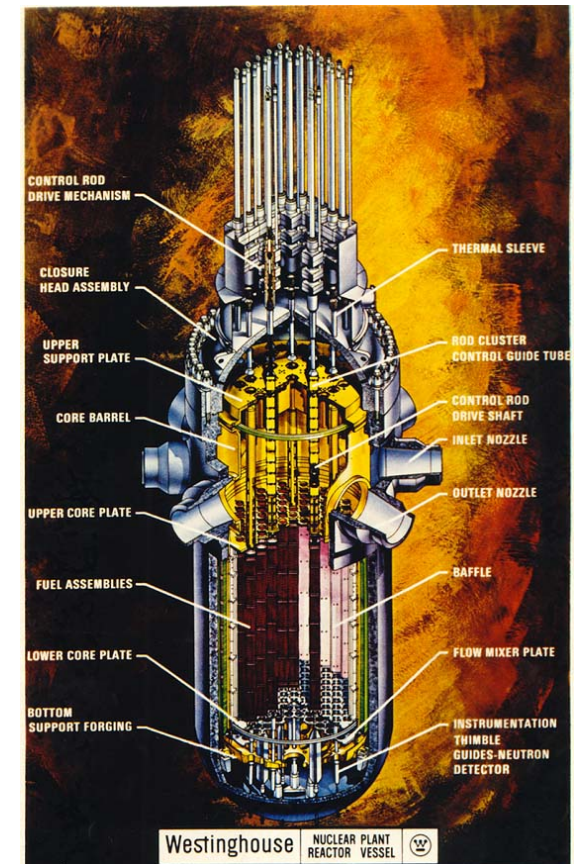
Coupled Neutron / Nuclide and Temperature/ Fluid Field Equations

- 💡 Neutron Transport Equation (Boltzmann)

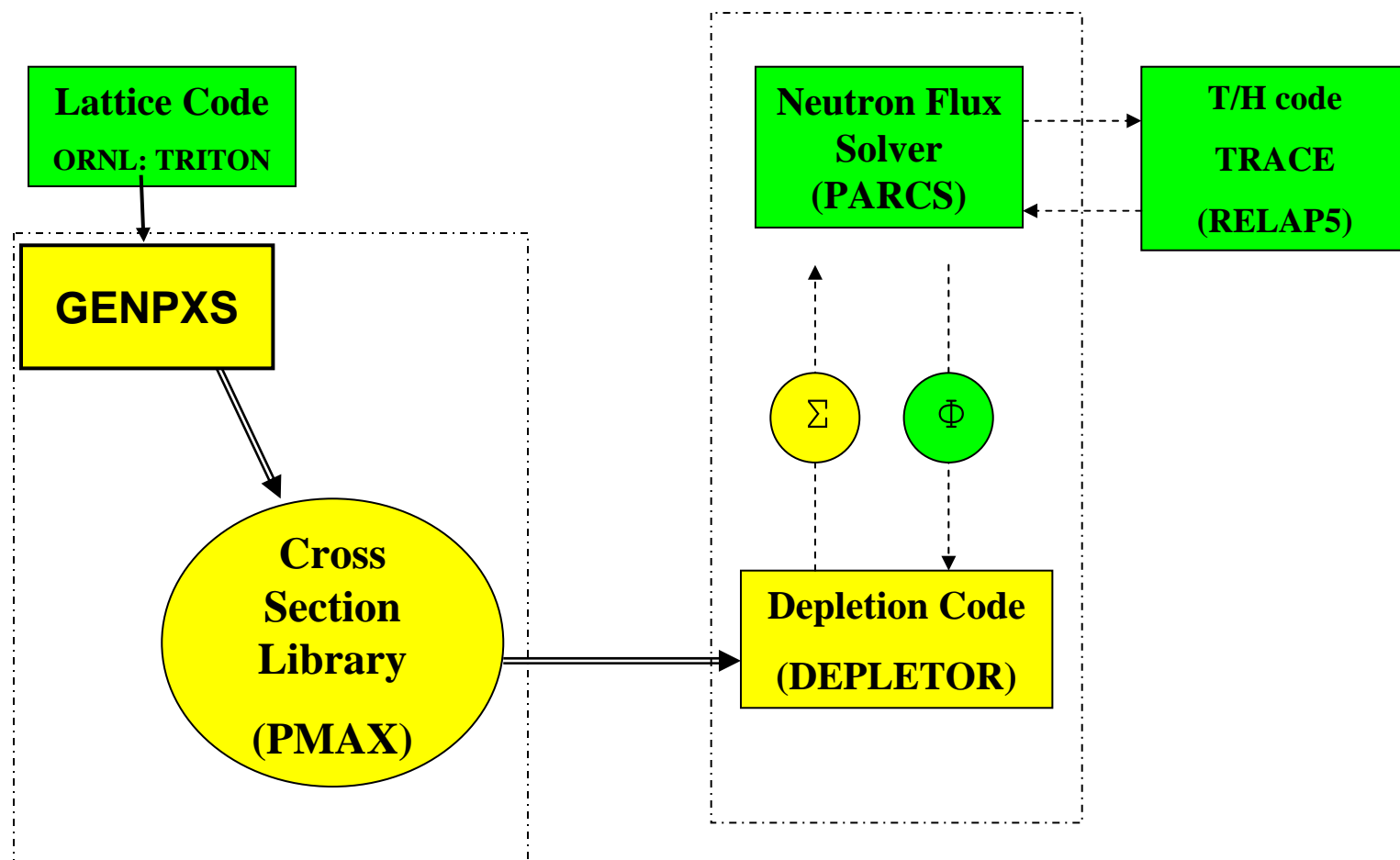
$$\frac{1}{v} \frac{\partial \phi}{\partial t} + \Omega \cdot \nabla \phi(r, E, \Omega, t) + \Sigma_t(r, E) \phi(r, E, \Omega, t) = \frac{1}{4\pi} S_f(r, E, t) \\ + \int \int_{\Omega E} \Sigma_s(r, E \rightarrow E', \Omega \rightarrow \Omega') \phi(r, E', \Omega', t) dE' d\Omega'$$

- Nuclide depletion equation (Bateman)

$$\frac{dN_A(t)}{dt} = -(\sigma_A^a \phi + \lambda_A) N_A(t) + \sigma_C^\gamma \phi N_c(t) + \lambda_B N_B(t)$$



U.S. NRC Coupled Code System



Coupling of Neutronics and Thermal-Hydraulics

- Neutron Cross Section Model

$$\Sigma(\alpha, Tf, Tm, Dm, Sb) = \Sigma^r + \alpha \Delta \Sigma^{cr} + \frac{\partial \Sigma}{\partial \sqrt{Tf}} \Delta \sqrt{Tf} + \frac{\partial \Sigma}{\partial Tm} \Delta Tm + \frac{\partial \Sigma}{\partial Dm} \Delta Dm + \frac{\partial \Sigma}{\partial Sb} \Delta Sb + \frac{\partial^2 \Sigma}{\partial Dm^2} (\Delta Dm)^2$$

$$\Delta \Sigma^{cr} = \Delta \Sigma^{cr}(BU, HIS1, HIS2)$$

$$\frac{\partial \Sigma}{\partial \sqrt{Tf}} = \frac{\partial \Sigma}{\partial \sqrt{Tf}}(\sqrt{Tf}, BU, HIS1, HIS2)$$

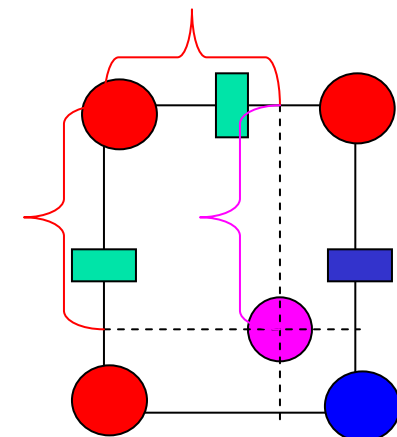
$$\frac{\partial \Sigma}{\partial Dm} = \frac{\partial \Sigma}{\partial Dm}(Dm, BU, HIS1, HIS2)$$

$$\frac{\partial \Sigma}{\partial Sb} = \frac{\partial \Sigma}{\partial Sb}(Sb, BU, HIS1, HIS2)$$

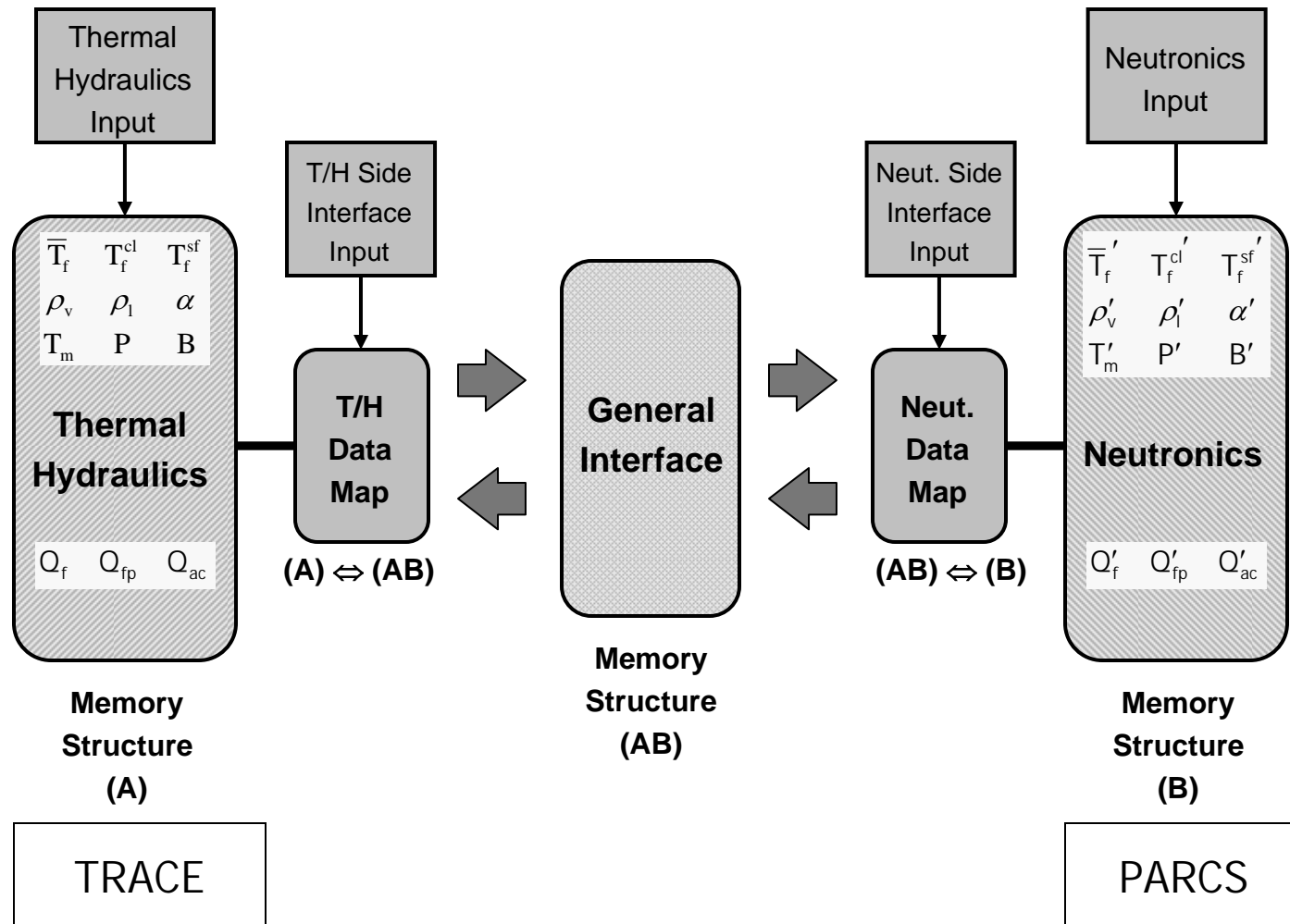
$$\frac{\partial \Sigma}{\partial Tm} = \frac{\partial \Sigma}{\partial Tm}(Tm, BU, HIS1, HIS2)$$

$$\frac{\partial^2 \Sigma}{\partial Dm^2} = \frac{\partial^2 \Sigma}{\partial Dm^2}(Dm, BU, HIS1, HIS2)$$

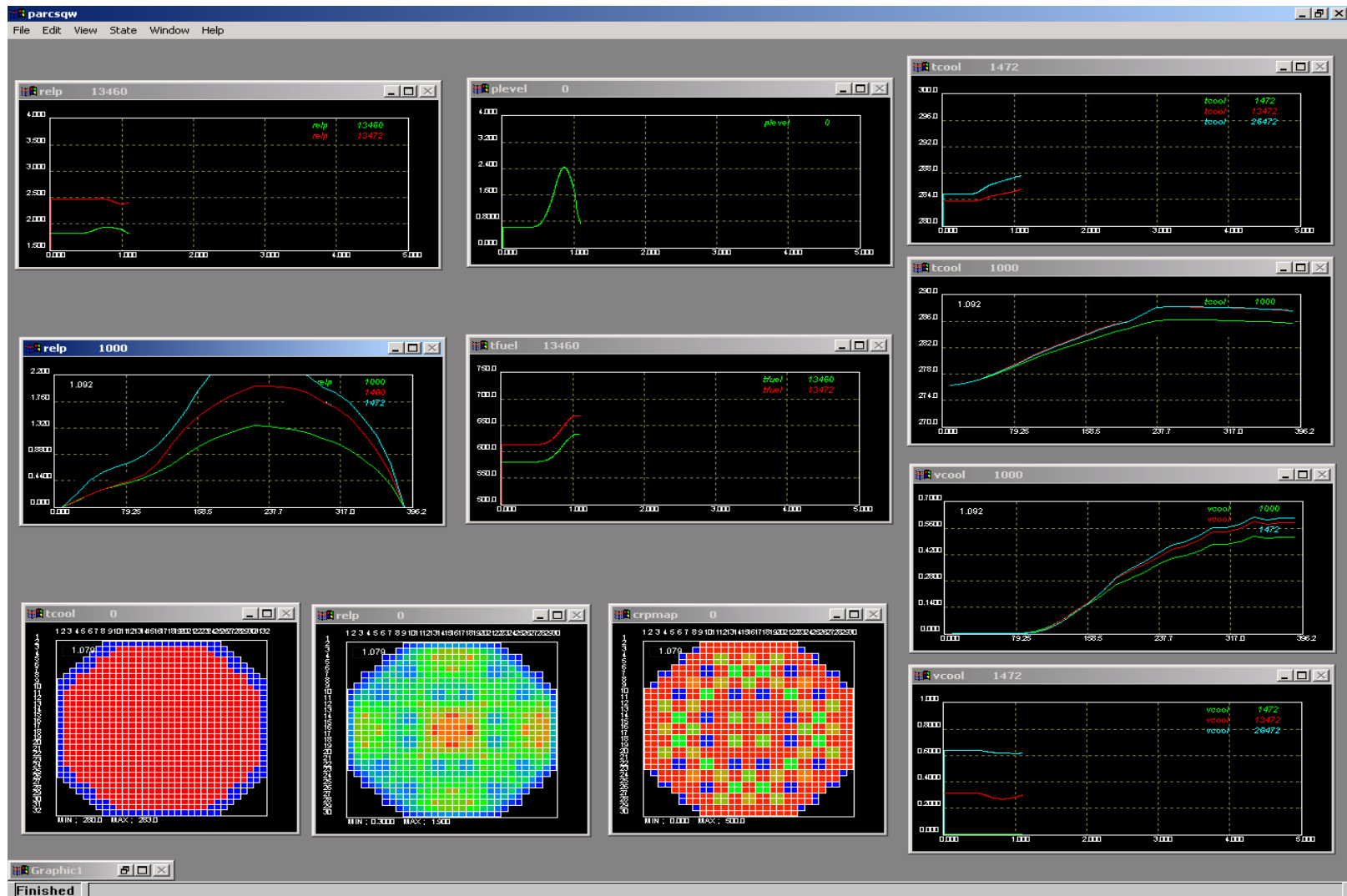
- Partials obtained by piecewise linear interpolation
- Burnup and burnup “history” dependence



Coupled TH/Neutronics Codes



U.S. NRC Coupled Code: TRACE/PARCS

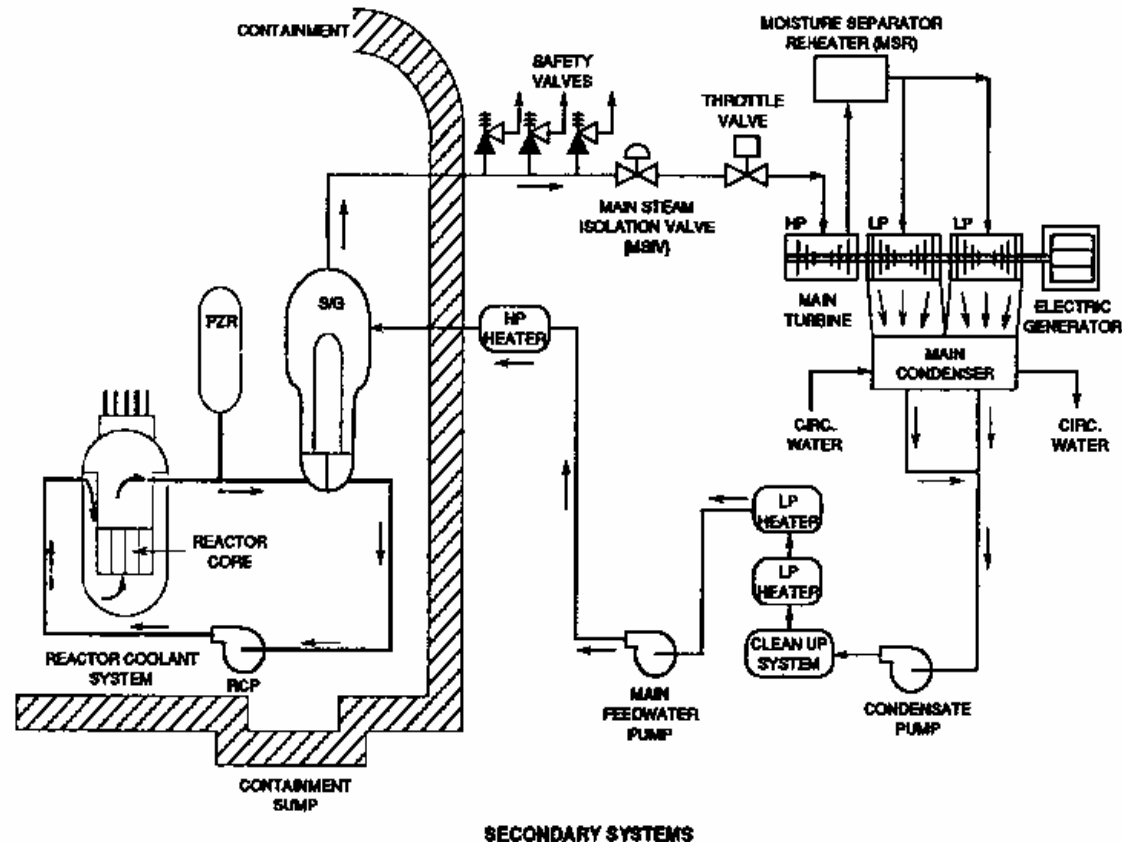


Coupled Code Assessment

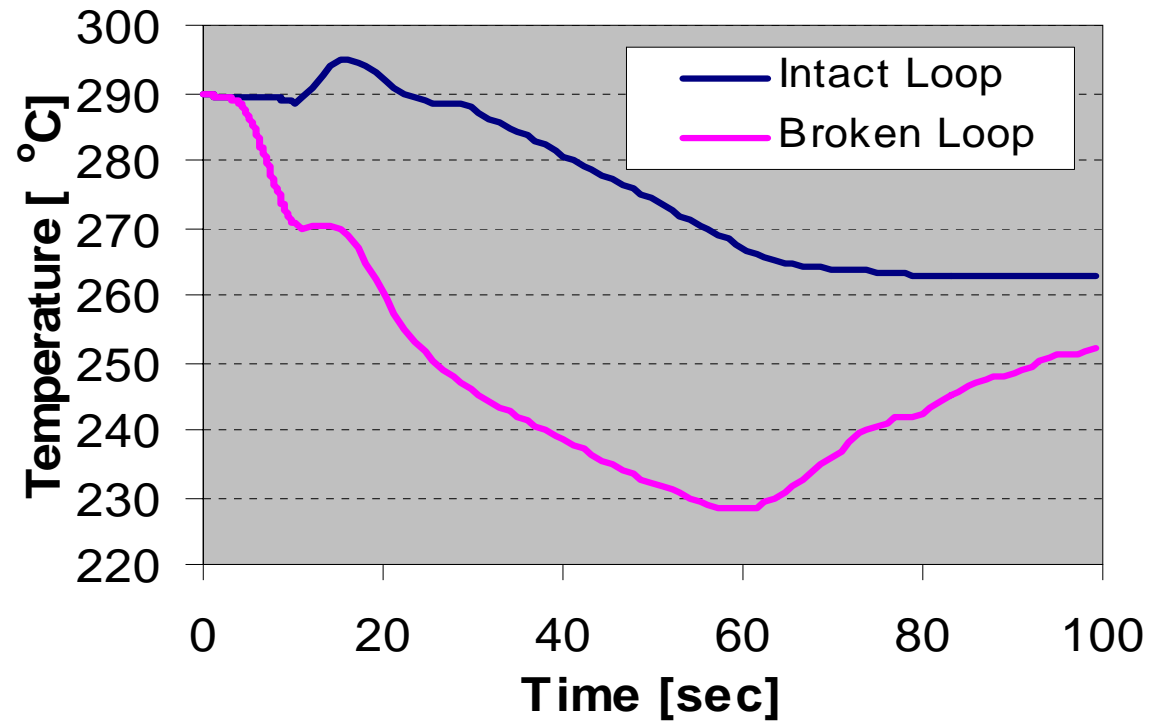
- Pressurized Water Reactor
 - Main Steam Line Break
 - Control Rod Drive Cracking
- Boiling Water Reactor
 - Peach Bottom Turbine Trip Test
 - Ringhalls Flow Instability

Nuclear Reactor Transient Analysis: Main Steam Line Break

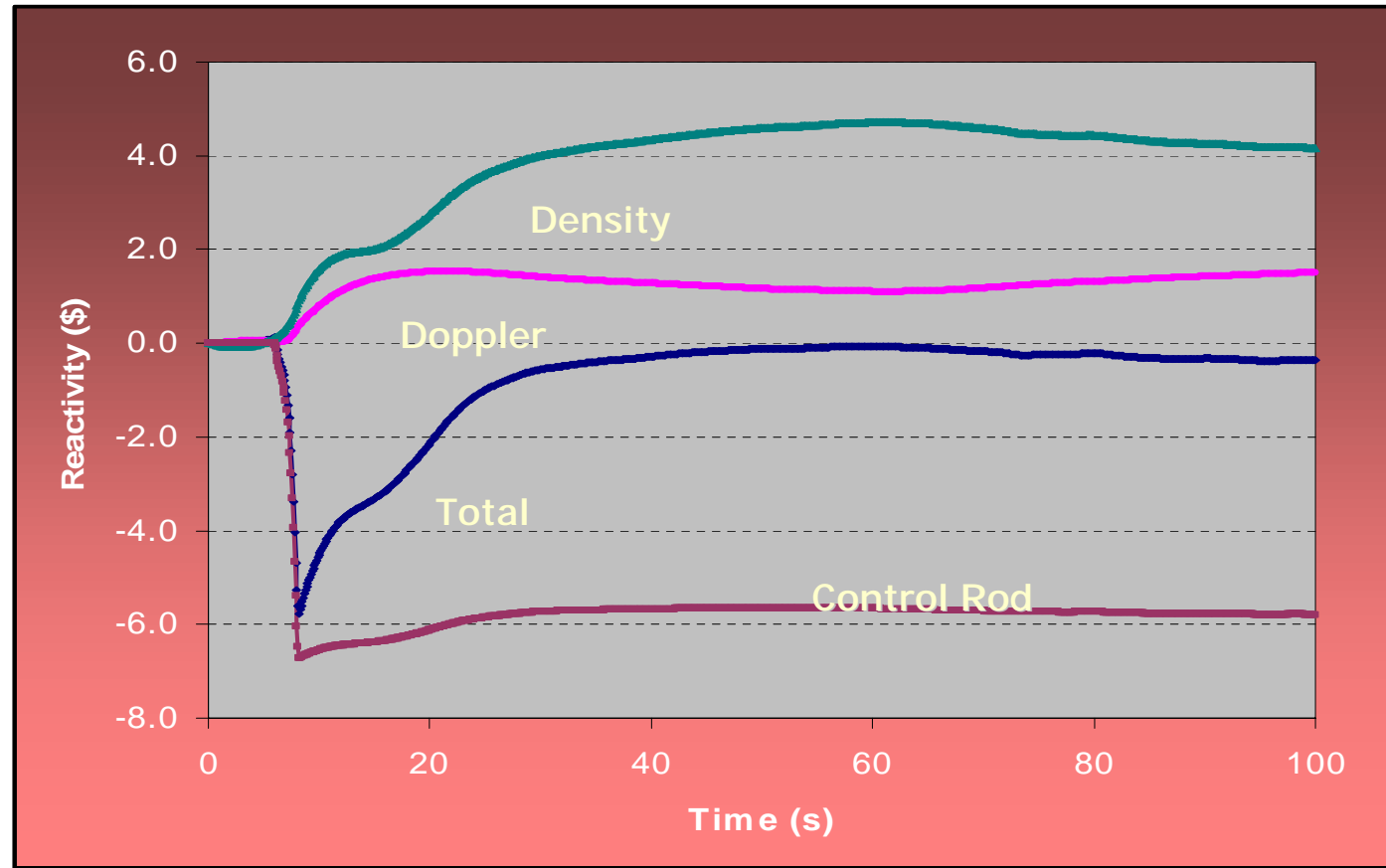
PWR Plant
Schematic



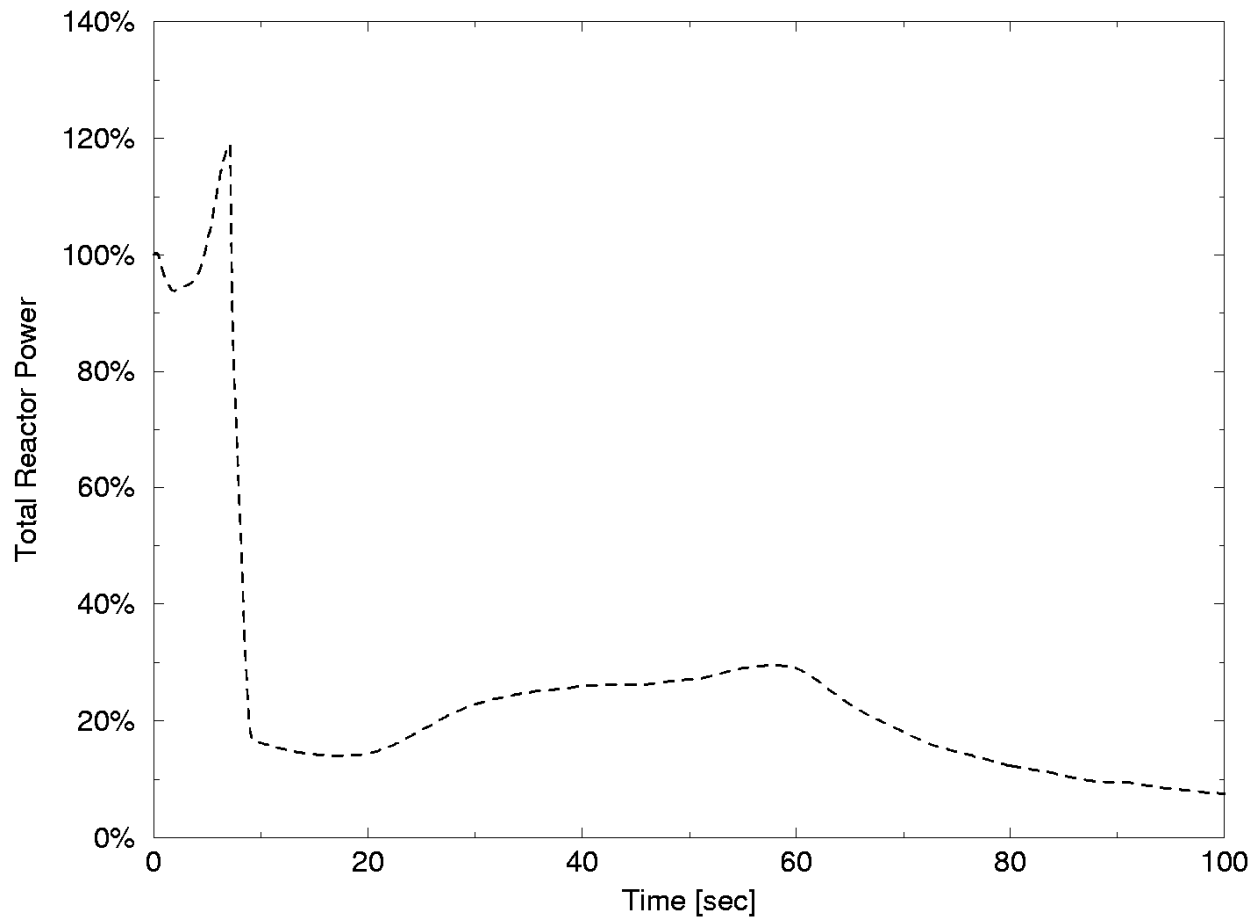
Main Steam Line Break Transient: Core Coolant Temperature



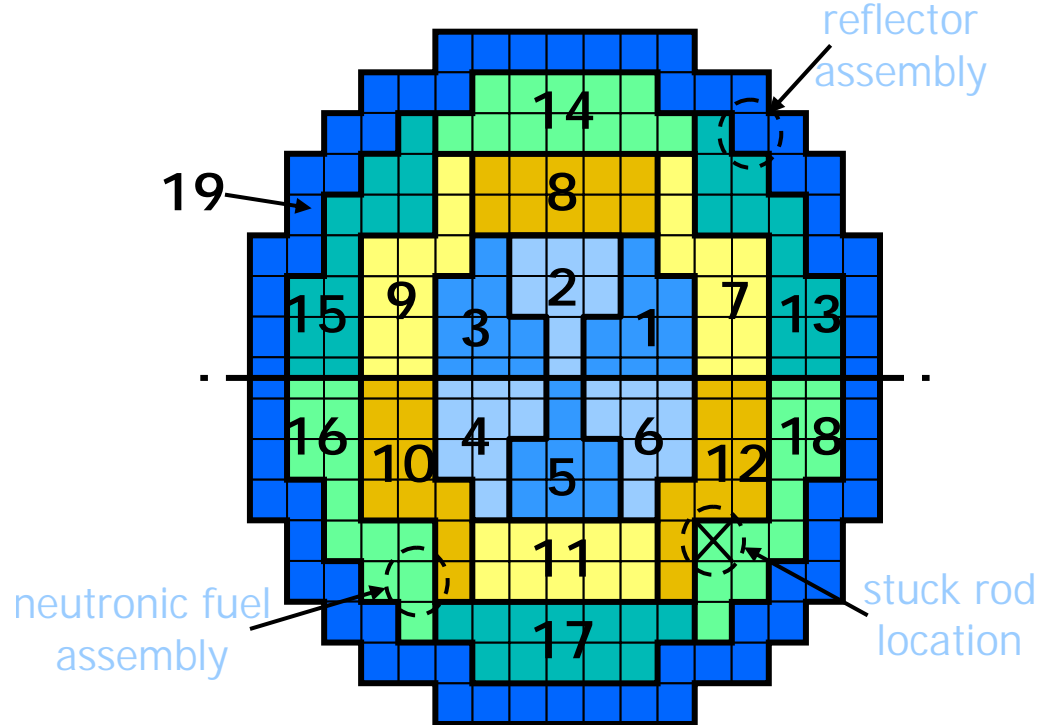
MSLB: Reactivity Components



Main Steam Line Break Analysis: Core Average Power

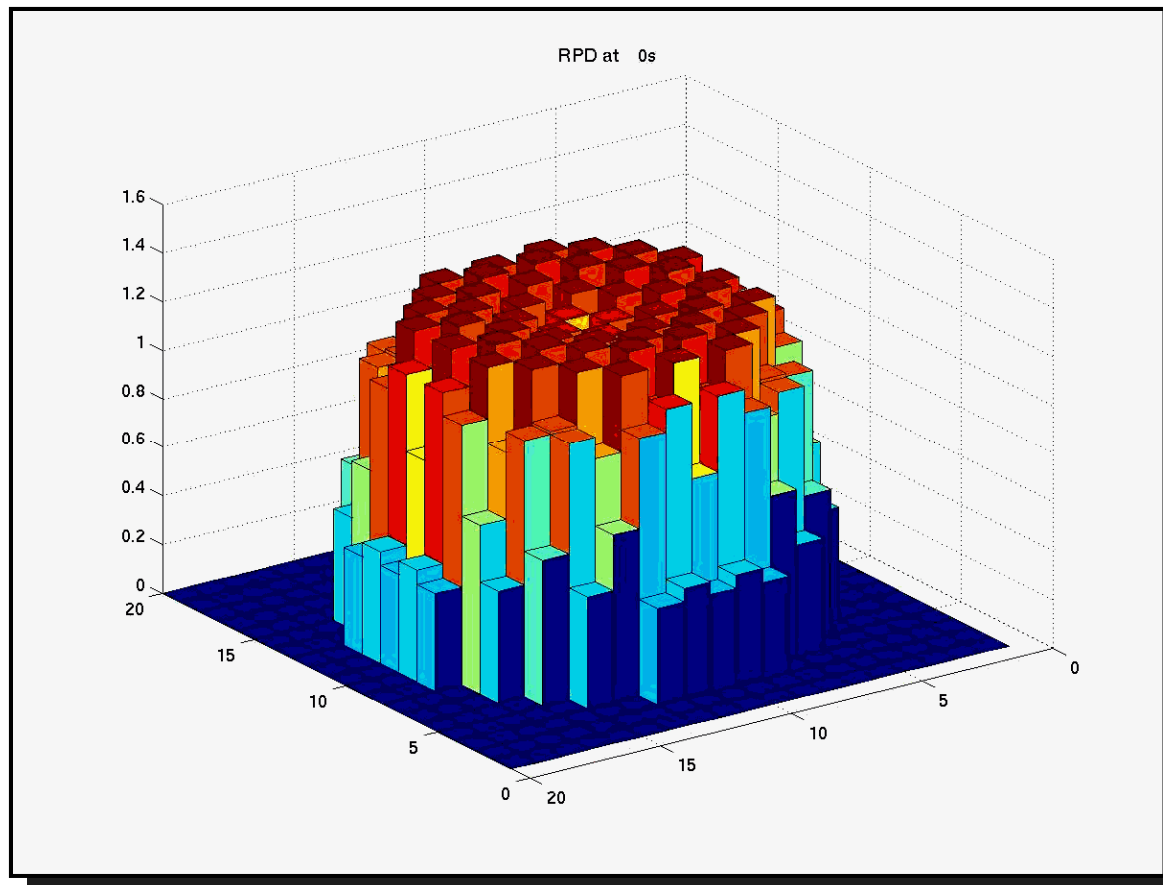


Core Neutronics Model



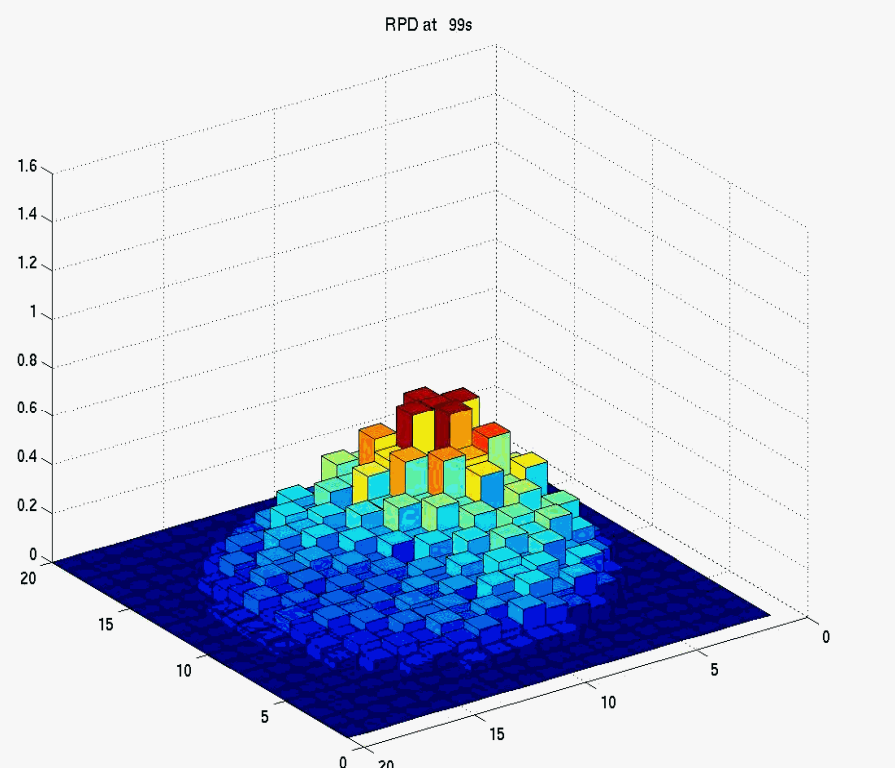
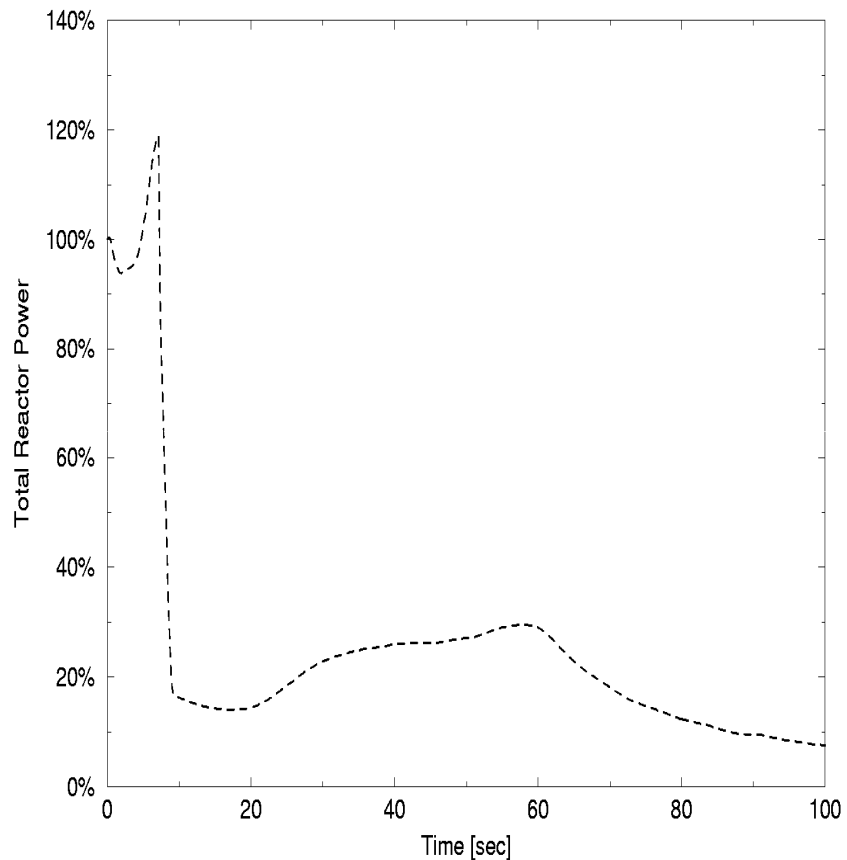
Three-Dimensional Analysis of Main Steam Line Break

■ Initial Steady-State

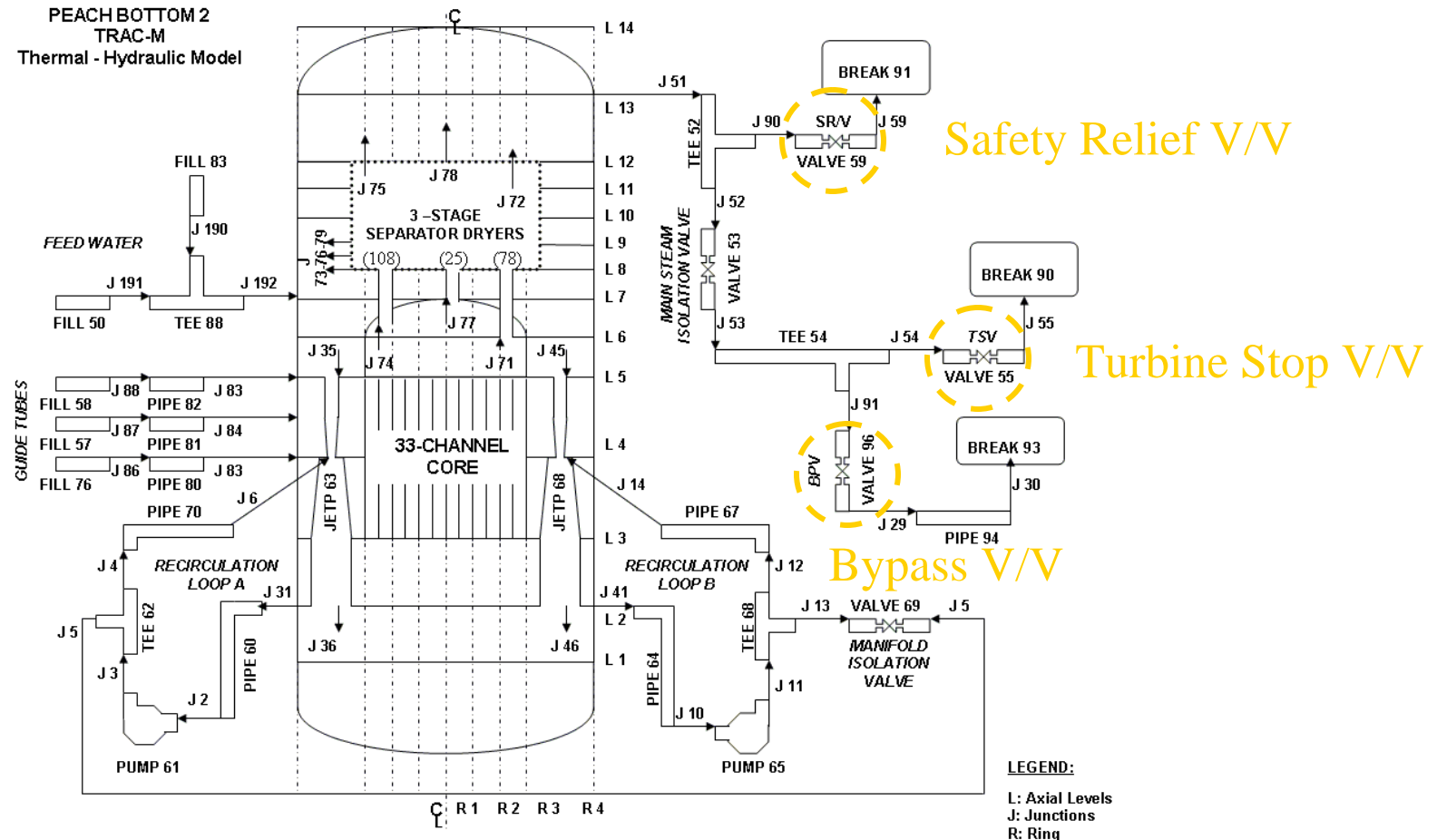


MSLB Transient Analysis

■ Radial Power Evolution



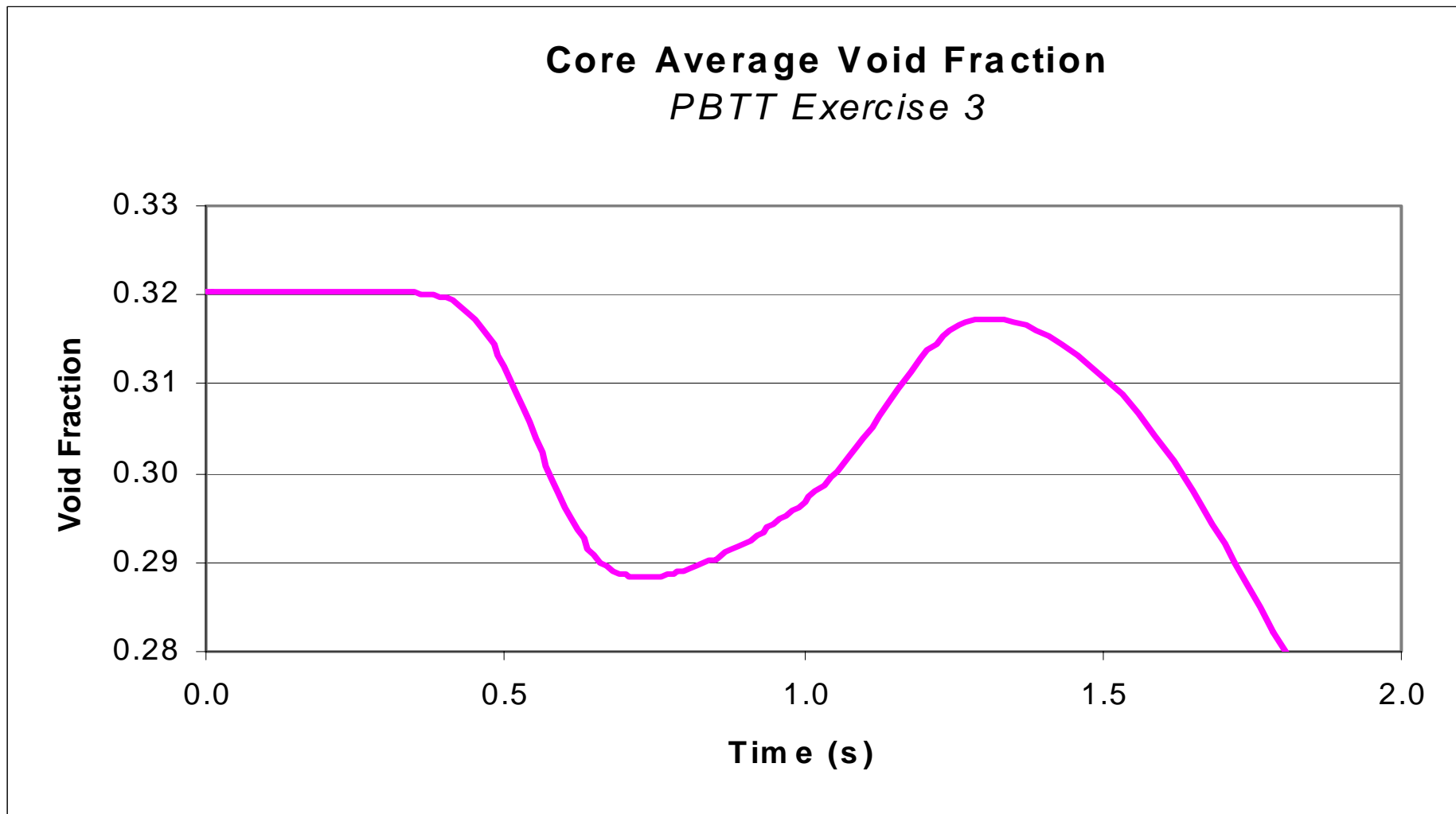
BWR Coupled Code Assessment: Peach Bottom Turbine Trip Benchmark



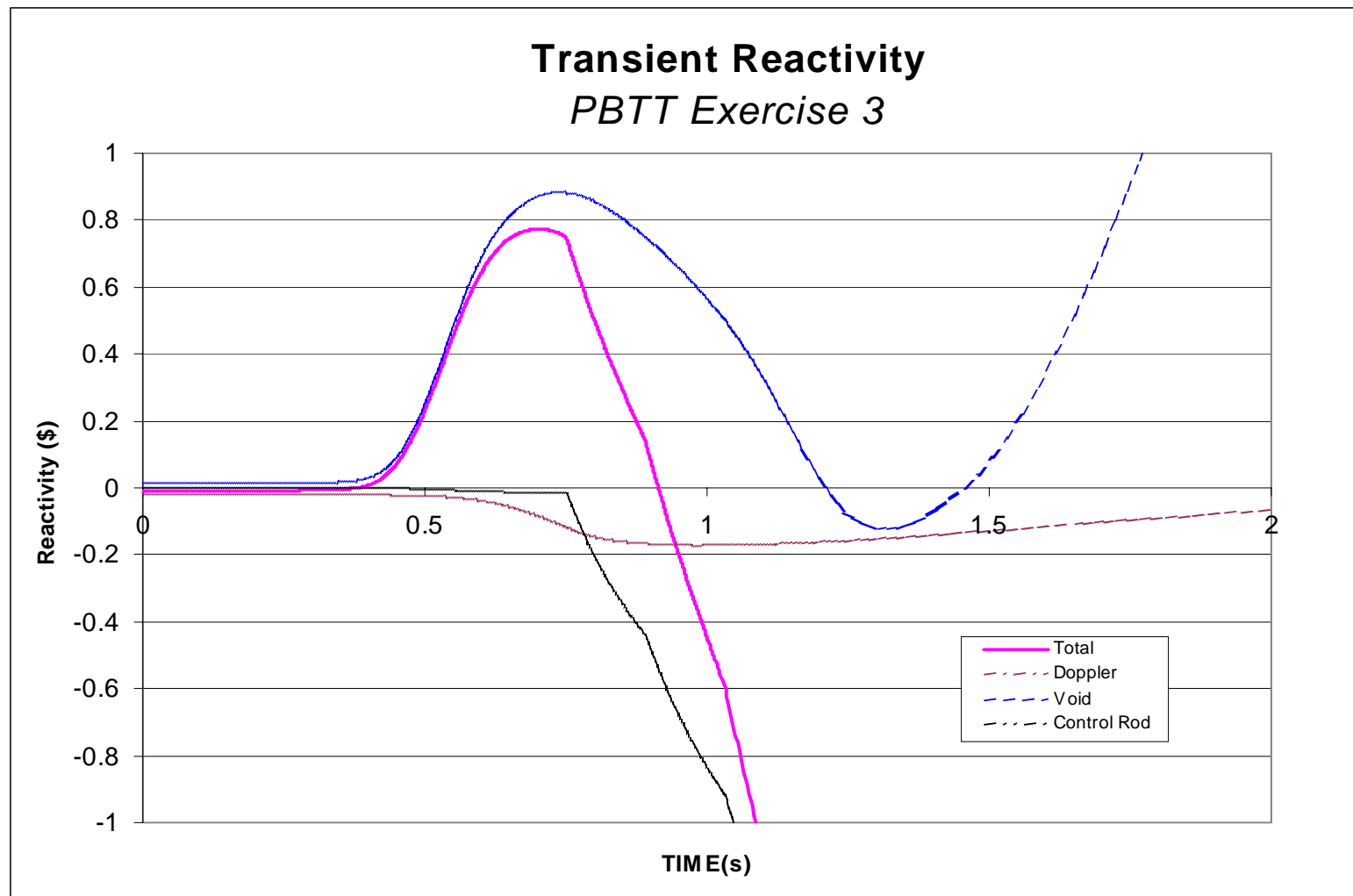
Peach Bottom Turbine Trip Transient Scenario

- Sudden Closure of the Turbine Stop Valve (TSV)
- The Pressure Oscillation Generated in the Main Steam Piping Propagates With Relatively Little Attenuation Into the Reactor Core
- The Core Pressure Induced Oscillations Result in Dramatic Changes in the Core Void Distribution and Fluid Flow
- The Magnitude of the Neutron Flux is Strongly Affected by the Initial Rate of Pressure Rise Caused by the Pressure Oscillation and has a Strong Spatial Variation

Void Fraction During Transient

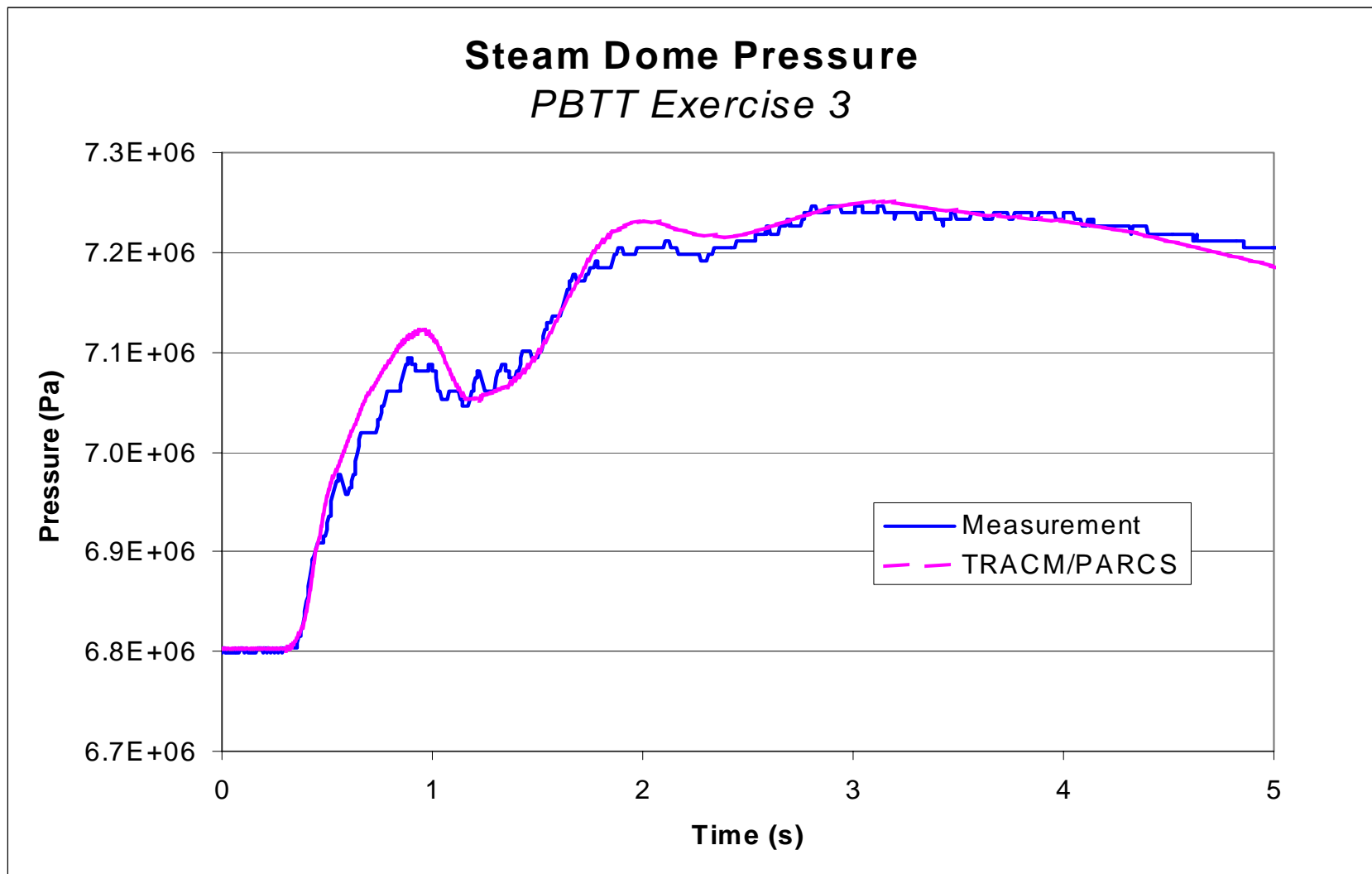


Core Reactivity During Transient

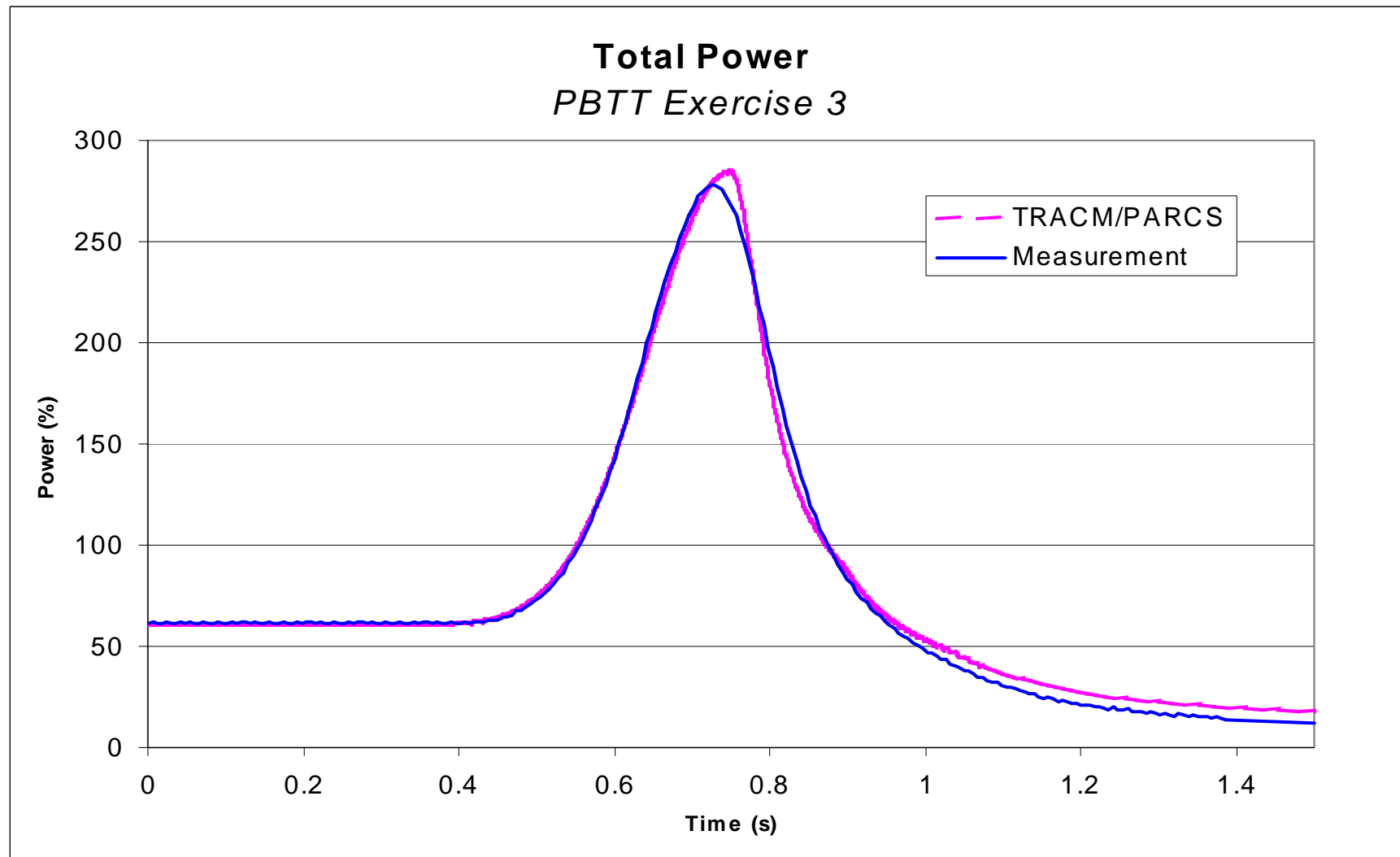


TRANSIENT RESULTS

Steam Dome Pressure

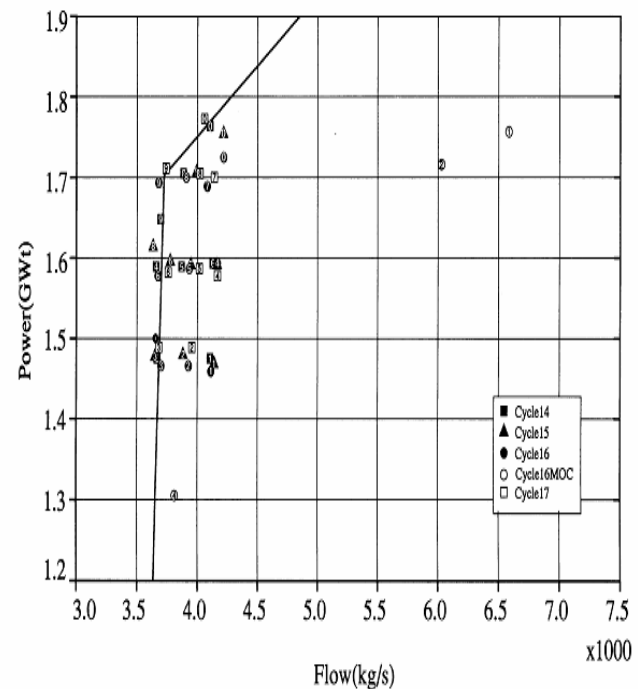


PBTT Transient Results



Ringhals Stability Benchmark

- Benchmark to validate the Coupled Codes' Predictive Capabilities for BWR Stability Analysis
- Code-to-Code and Code-to-Experimental Data Comparisons
- The PSU/PURDUE Project currently includes Two Measured Point Cases from the RH1 Benchmark:
 - Point 9 of Cycle 14 (C14P9): Regional Mode of Oscillations
 - Point 10 of Cycle 14 (C14P10): Global Mode of Oscillation



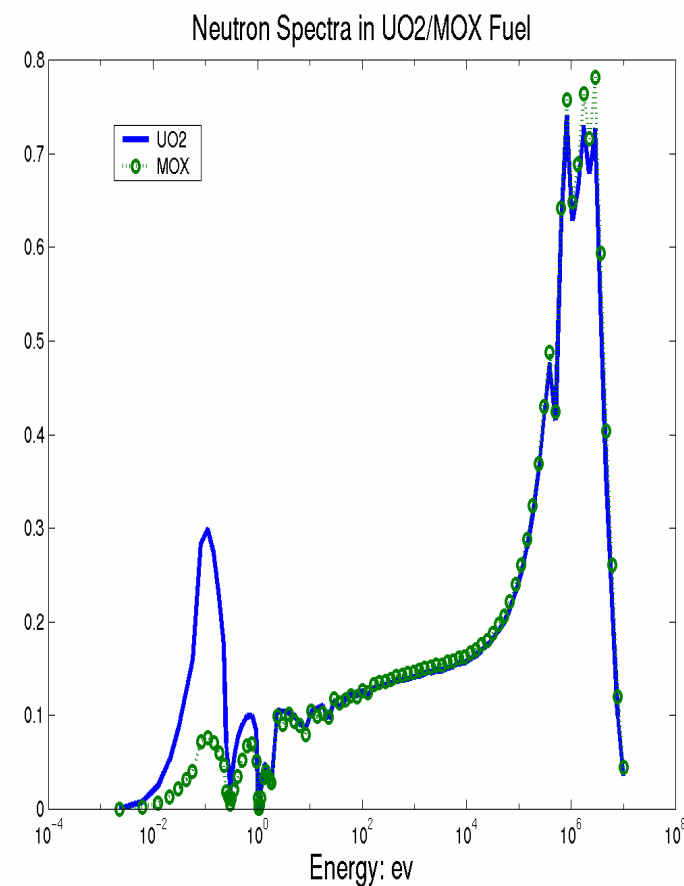
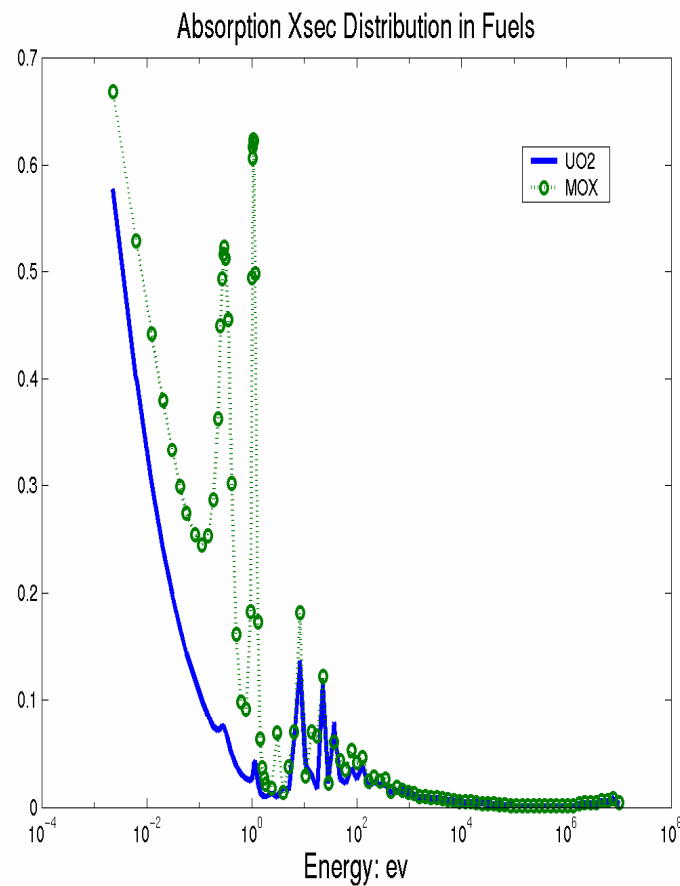
Advanced Reactors

- Recent emphasis has been on addressing GENIII+/GENIV licensing concerns:
 - ESBWR
 - PBMR / HTR
 - ACR-700
- Also an effort has been underway during the last three years to assess neutronics methods for MOX fuel analysis as part of the LWR PU Disposition program

Weapons Grade Plutonium Disposition in the U.S.

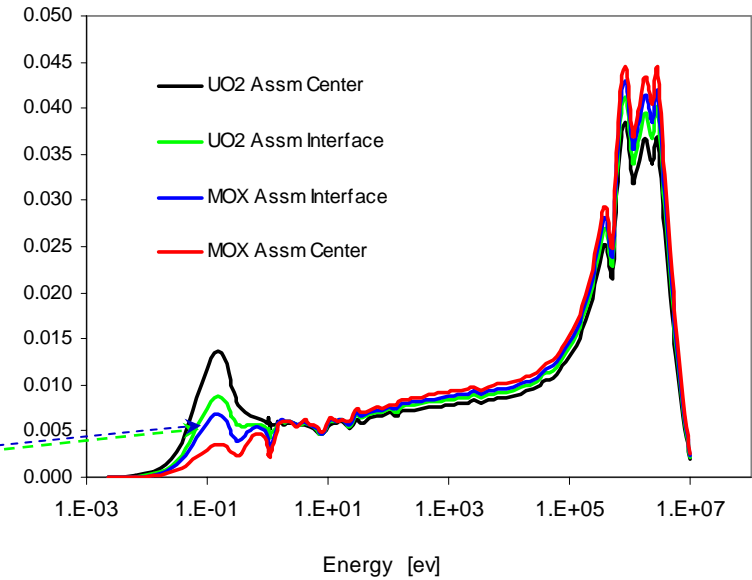
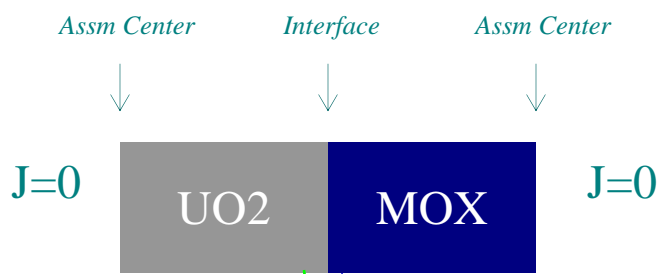
- In 1998 the decision was made to dispose of excess Plutonium from dismantled weapons by irradiation in selected U.S. PWRs
- Because the properties of Fissile PU and U are very different, modifications were required to the PARCS code

Challenges Presented by MOX Fuel

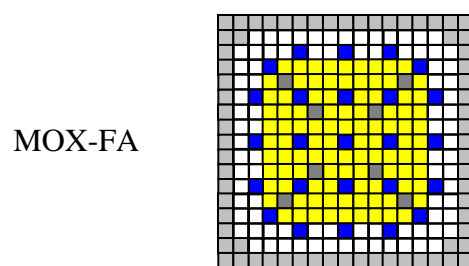
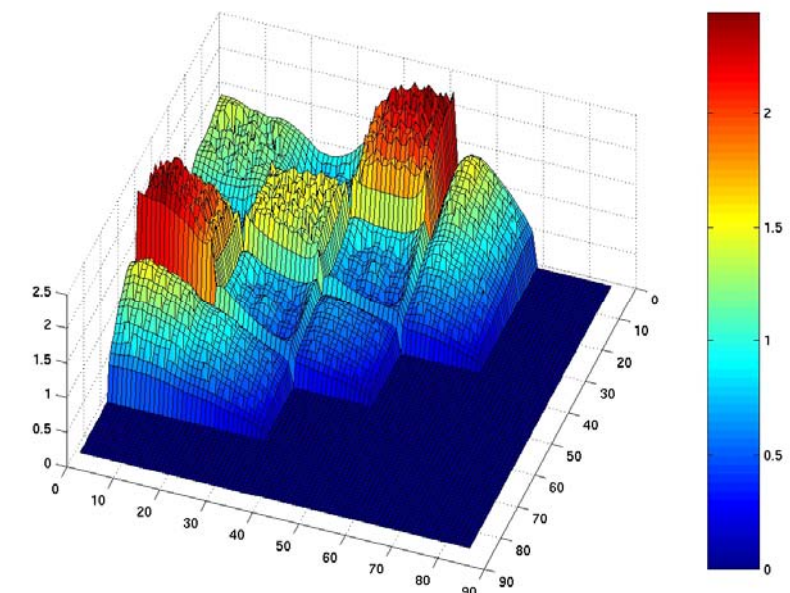
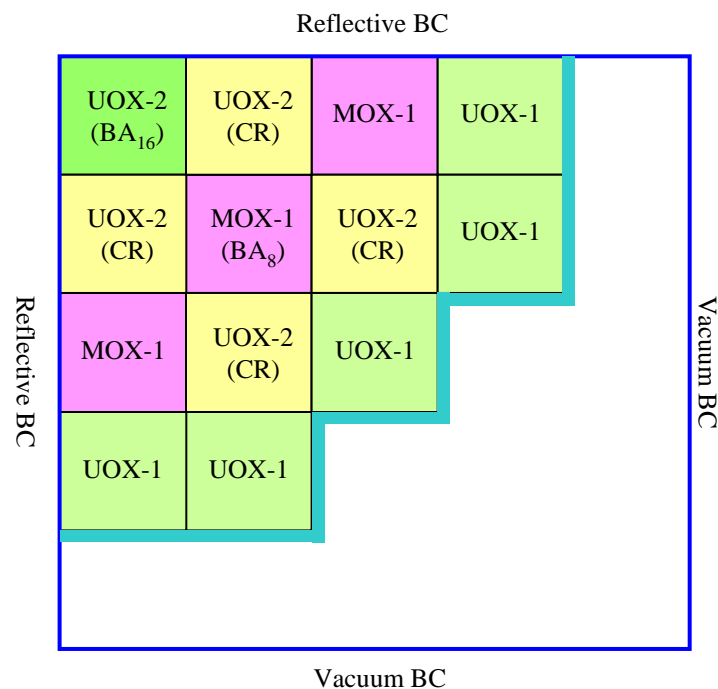


Challenges Presented by MOX Fuel

■ 1-D Configuration



MOX LWR Benchmark Problem



“AD HOC” Methods

- Leakage Correlation

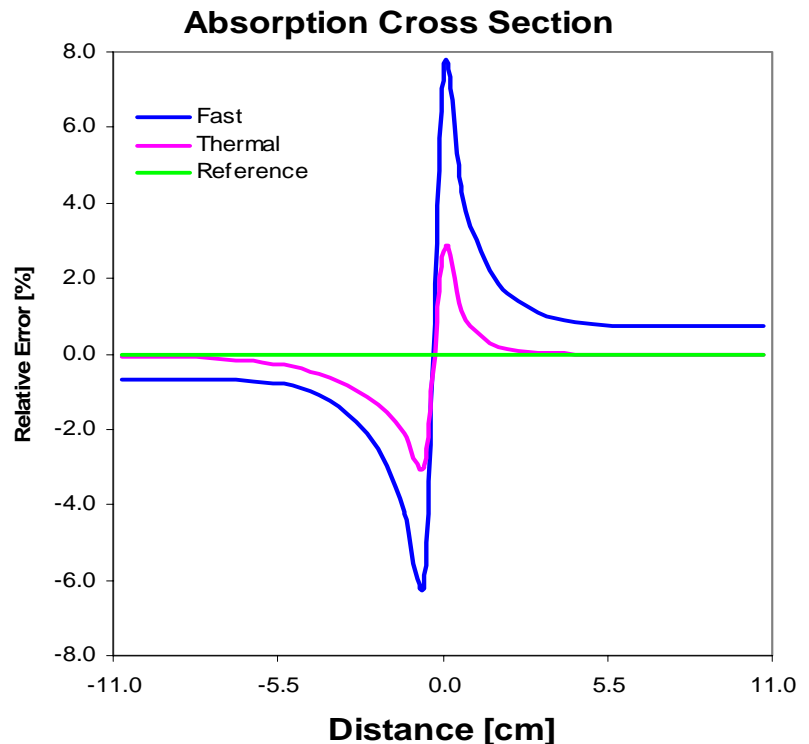
$$\frac{\sum_{\alpha 1}^B(x) - \sum_{\alpha 1}^{SA}(x)}{\sum_{\alpha 1}^{SA}(x)} = B_{\alpha 1} \left[\frac{-D_1 \nabla^2 \phi_1(x)}{\sum_{\alpha 1}^{SA} \phi_1(x) + \sum_{21}^{SA} \phi_1(x)} \right], \quad B_{\alpha 2} = 0$$

- Spectral Correlation

$$\frac{\sum_{\alpha g}^S(x) - \sum_{\alpha g}^B(x)}{\sum_{\alpha g}^B(x)} = \pm C_{\alpha g} \left| \frac{\Gamma(x) - \Gamma^{SA}}{\Gamma^{SA}} \right|^{\beta_{\alpha g}}, \quad \Gamma(x) \equiv \frac{\phi_2(x)}{\phi_1(x)}$$

Studsvik (Duke Power)

SPATIAL CROSS SECTION



Methods Upgrade In PARCS

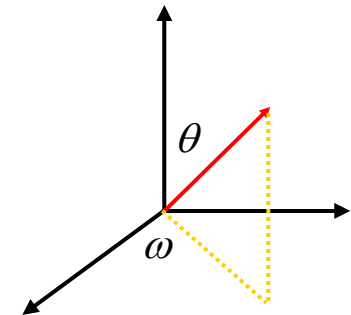
$$\begin{aligned} & \frac{1}{\nu} \frac{\partial}{\partial t} \psi(r, \Omega, E, t) + \Omega \cdot \nabla \psi(r, \Omega, E, t) + \Sigma(r, E) \psi(r, \Omega, E, t) \\ &= \int d\Omega' \int dE' \Sigma_s(r, \Omega' \rightarrow \Omega, E' \rightarrow E) \psi(r, \Omega', E', t) + S(r, \Omega, E, t) \end{aligned}$$

- **Fundamental approach to reduce errors for MOX-loaded cores**
 - Space : FA heterogeneity (pin-by-pin configuration)
 - Energy : Multigroup
 - Angle : Transport method (SP_3)

SP_N Approximation

- 1-D P_N Equation

$$\psi(x, \mu, E) = \sum_{n=0}^N \left(\frac{2n+1}{2} \right) \phi_n(x, E) P_n(\mu)$$



$$\frac{(n+1)}{(2n+1)} \frac{\partial \phi_{n+1}(x, E)}{\partial x} + \frac{n}{(2n+1)} \frac{\partial \phi_{n-1}(x, E)}{\partial x} + \Sigma_t \phi_n(x, E) = \int_0^\infty dE' \Sigma_{sn}(x, E' \rightarrow E) \phi_n(x, E') + s_n(x, E)$$

$$\frac{\partial \phi_n(x, E)}{\partial x} \quad \xrightarrow{\text{green arrow}} \quad \nabla \cdot \phi_n(r, E) \quad n = \text{even}$$

$$\frac{\partial \phi_n(x, E)}{\partial x} \quad \xrightarrow{\text{green arrow}} \quad \nabla \phi_n(r, E) \quad n = \text{odd}$$

- Extension of 1-Dimensional P_N to Multi-dimensional Geometry

Origin of SP₃ Approximation

- Extrapolation of 1-Dimensional P_N to Multidimensional Geometry

$$\frac{(n+1)}{(2n+1)} \frac{\partial \phi_{n+1}(x, E)}{\partial x} + \frac{n}{(2n+1)} \frac{\partial \phi_{n-1}(x, E)}{\partial x} + \Sigma_t \phi_n(x, E) = \int_0^\infty dE' \Sigma_{sn}(x, E' \rightarrow E) \phi_n(x, E') + s_n(x, E)$$



$$\frac{(n+1)}{(2n+1)} \nabla \phi_{n+1}(r, E) + \frac{n}{(2n+1)} \nabla \phi_{n-1}(r, E) + \Sigma_t \phi_n(r, E) = \int_0^\infty dE' \Sigma_{sn}(r, E' \rightarrow E) \phi_n(r, E') + s_n(r, E)$$

- Even moments: scalars operated on by gradient
- Odd moments: vectors operated on by divergence
- Limitation: strong multidimensional effect can not be properly considered
 - Voids
 - Streaming regions
 - Geometrically complex and spatially inhomogeneous regions

Time-dependent SP₃ Equation

- Governing Equations

$$\frac{1}{v} \frac{\partial \phi_{0g}}{\partial t} + \nabla \cdot \phi_{1g} + \Sigma_{rg} \phi_{0g} = s_{0g}$$

$$\frac{1}{v} \frac{\partial \phi_{1g}}{\partial t} + \frac{2}{3} \nabla \cdot \phi_{2g} + \frac{1}{3} \nabla \cdot \phi_{0g} + \Sigma_{trg} \phi_{1g} = 0$$

$$\frac{1}{v} \frac{\partial \phi_{2g}}{\partial t} + \frac{3}{5} \nabla \cdot \phi_{3g} + \frac{2}{5} \nabla \cdot \phi_{1g} + \Sigma_{tg} \phi_{2g} = 0$$

$$\frac{1}{v} \frac{\partial \phi_{3g}}{\partial t} + \frac{3}{7} \nabla \cdot \phi_{2g} + \Sigma_{tg} \phi_{3g} = 0$$

- Second-order Differential Equations

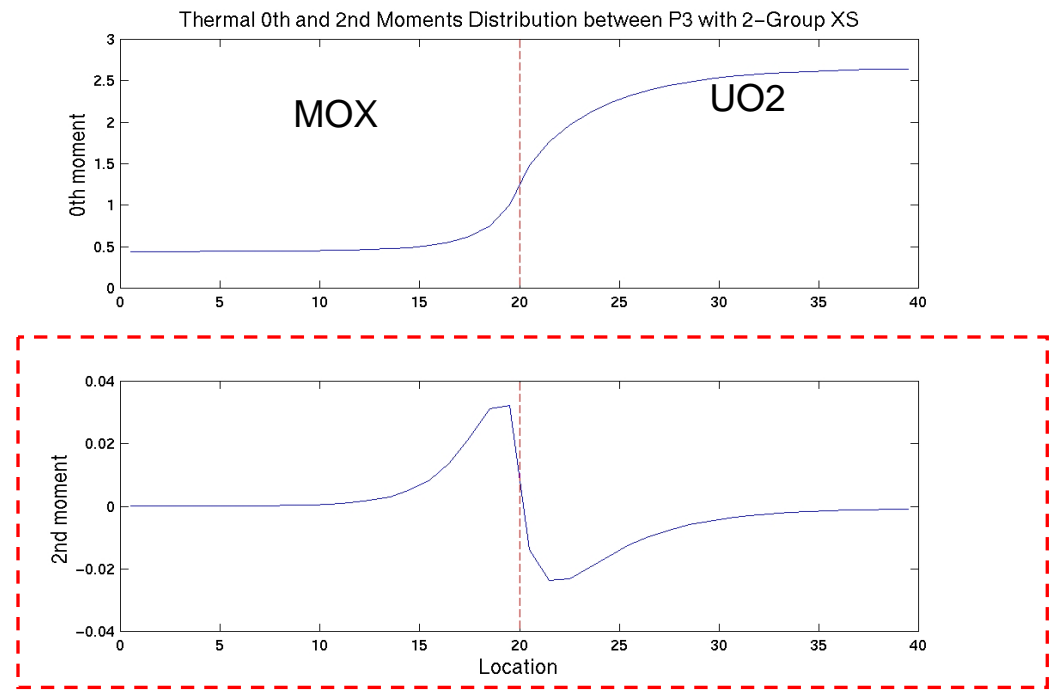
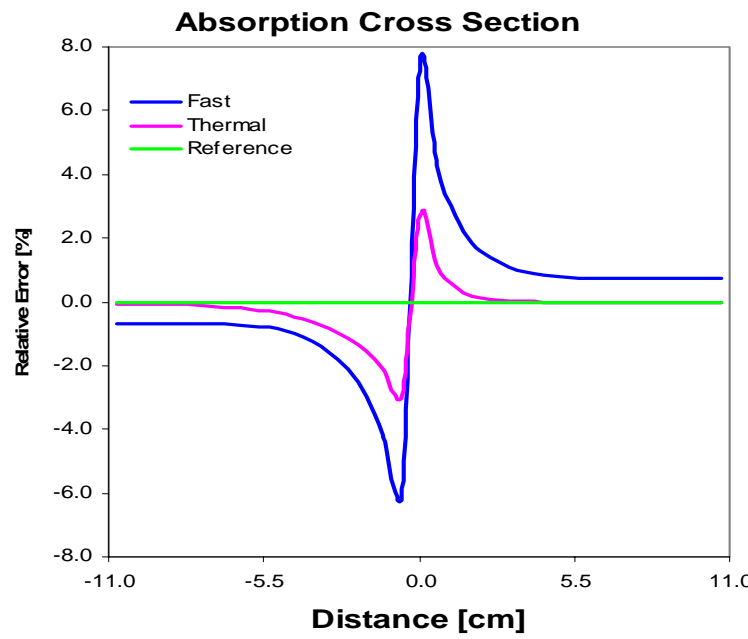
$$\begin{bmatrix} -D_1^* \nabla^2 + \Sigma_r^* & -2D_1^* \nabla^2 \\ -\frac{2}{5} D_1^* \nabla^2 & -\left(\frac{3}{5} D_3^* + \frac{4}{5} D_1^*\right) \nabla^2 + \Sigma_t^* \end{bmatrix} \begin{bmatrix} \phi_0^{n+1} \\ \phi_2^{n+1} \end{bmatrix} = \begin{bmatrix} q_0^n - 3D_1^* \nabla \cdot q_1^n + s_{0t}^{n+1} \\ q_2^n - \frac{6}{5} D_1^* \nabla \cdot q_1^n - \frac{7}{5} D_3^* \nabla \cdot q_3^n \end{bmatrix}$$

$$\left. \begin{array}{l} D_1^* \equiv \frac{1}{3\Sigma_{tr}^*} \\ D_3^* \equiv \frac{3}{7\Sigma_t^*} \\ \Sigma_\alpha^* = \Sigma_\alpha + \frac{1}{v\Delta t} \\ q_i^n = \frac{1}{v\Delta t} \phi_i^n \end{array} \right\} n = \text{time index}$$

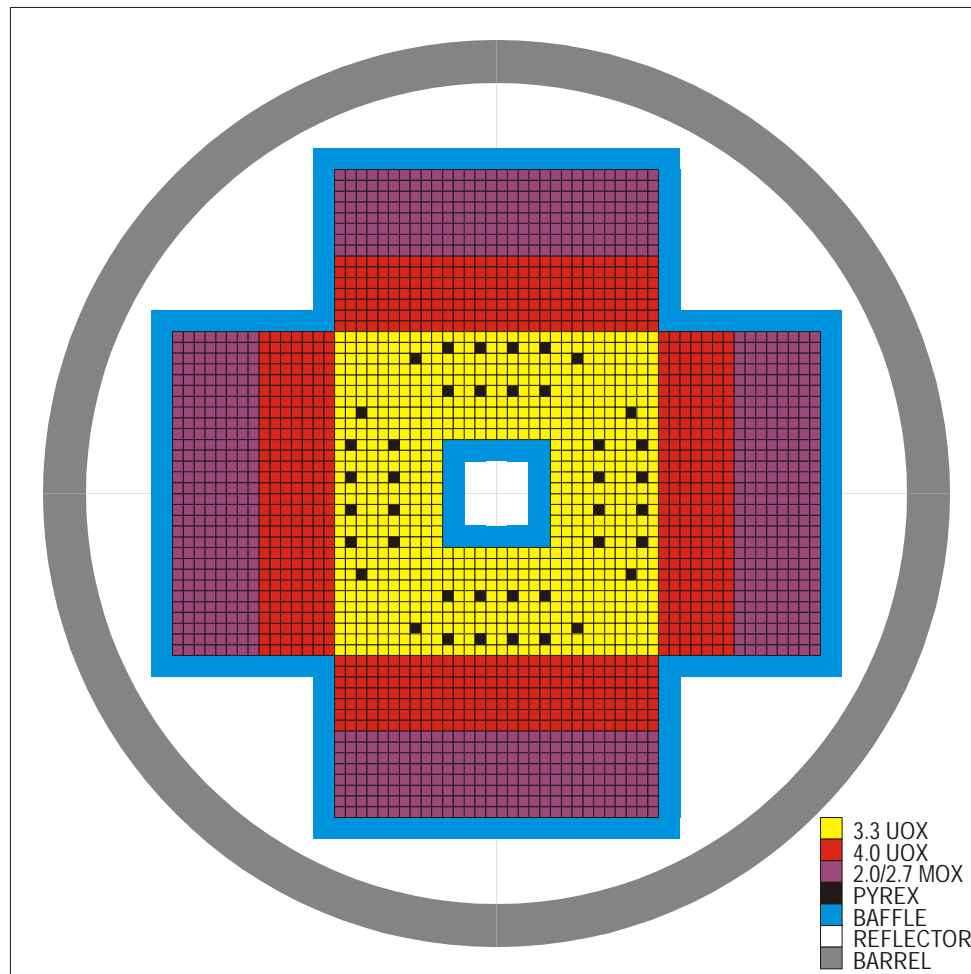
Characteristics of the 2nd Moment

- 2nd Moments of P₃ for Thermal Group in 1-D Geometry

$$-\left(\frac{3}{5}D_{3g} + \frac{4}{5}D_{1g}\right)\nabla^2\phi_{2g}(x) + \Sigma_{tg}\phi_{2g}(x) = -L_{0g}(x) \quad : \text{2}^{\text{nd}} \text{ moment Eq.}$$



Validation of MOX Methods with the VENUS-2 MOX Benchmark



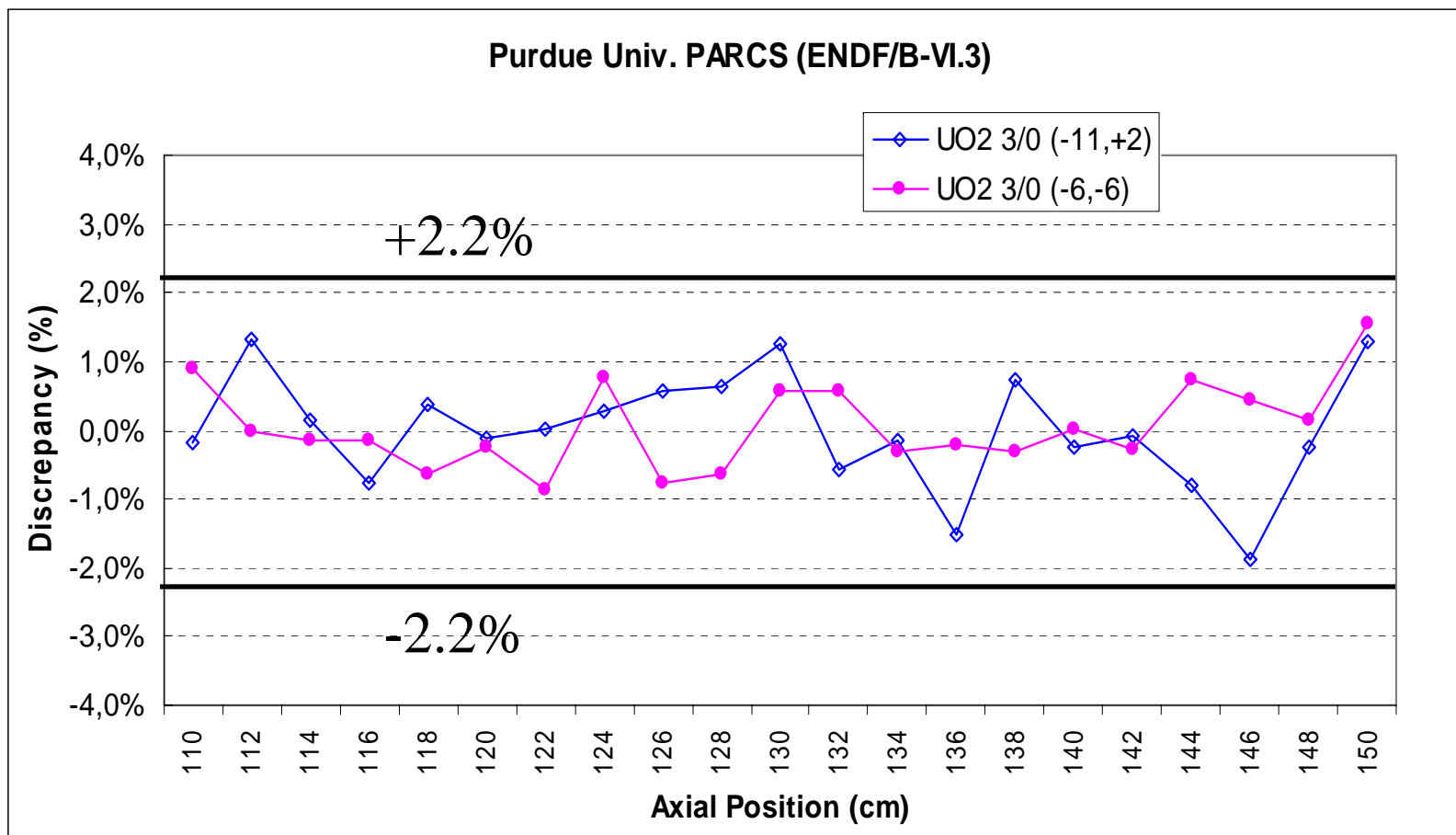
PARCS Results for VENUS-II Benchmark

Method	Group	Angle	Core k_{eff}	Pin Type %RMS			
				max % error	(peak pin % error)	MOX	All
Nodal	2	Diffusion	0.99990	7.26 -13.3(-9.6)	4.86 10.3 (0.4)	8.02 18.8 (3.6)	6.90 18.7 (0.4)
Fine Mesh*	2	Diffusion	0.99727	3.50 -6.2 (-2.4)	1.71 -3.9 (-3.9)	5.96 8.7 (1.8)	4.22 8.7 (-3.9)
		SP_3	1.00486	3.24 -5.7 (-2.2)	2.00 -4.5 (-4.5)	6.09 9.9 (0.6)	4.27 9.9(-4.5)
	8	Diffusion	0.99360	1.78 -3.1 (-1.0)	1.39 4.0 (-1.6)	3.22 5.6 (0.6)	2.33 5.6 (-1.6)
		SP_3	1.00284	1.80 -3.2 (-1.1)	1.55 4.4 (-2.2)	3.27 6.0 (-0.2)	2.39 6.0 (-2.2)

*4x4 mesh per pin

Note: comparison made to HELIOS reference.

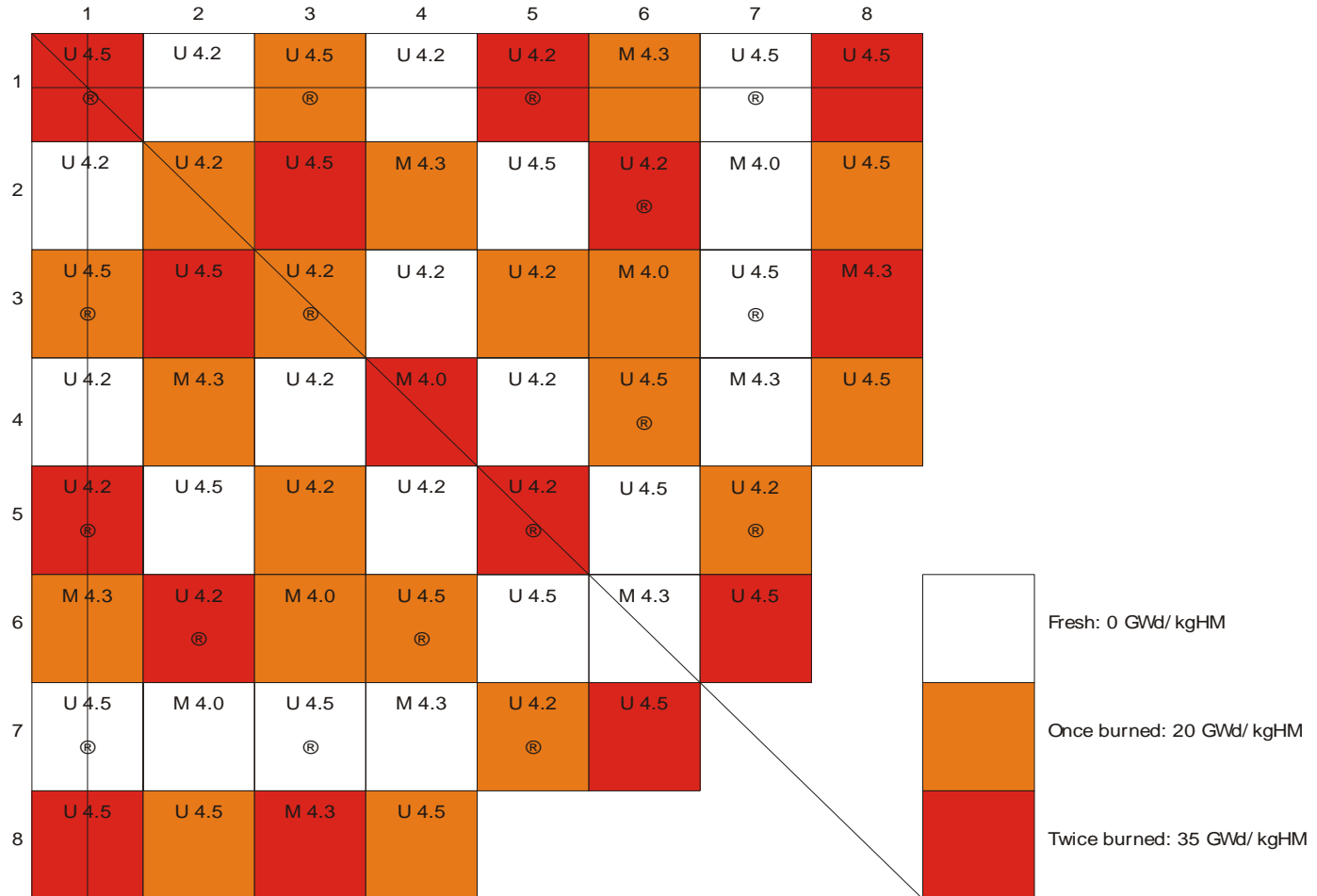
PARCS 3D Core Calculation Comparison to Measured Data



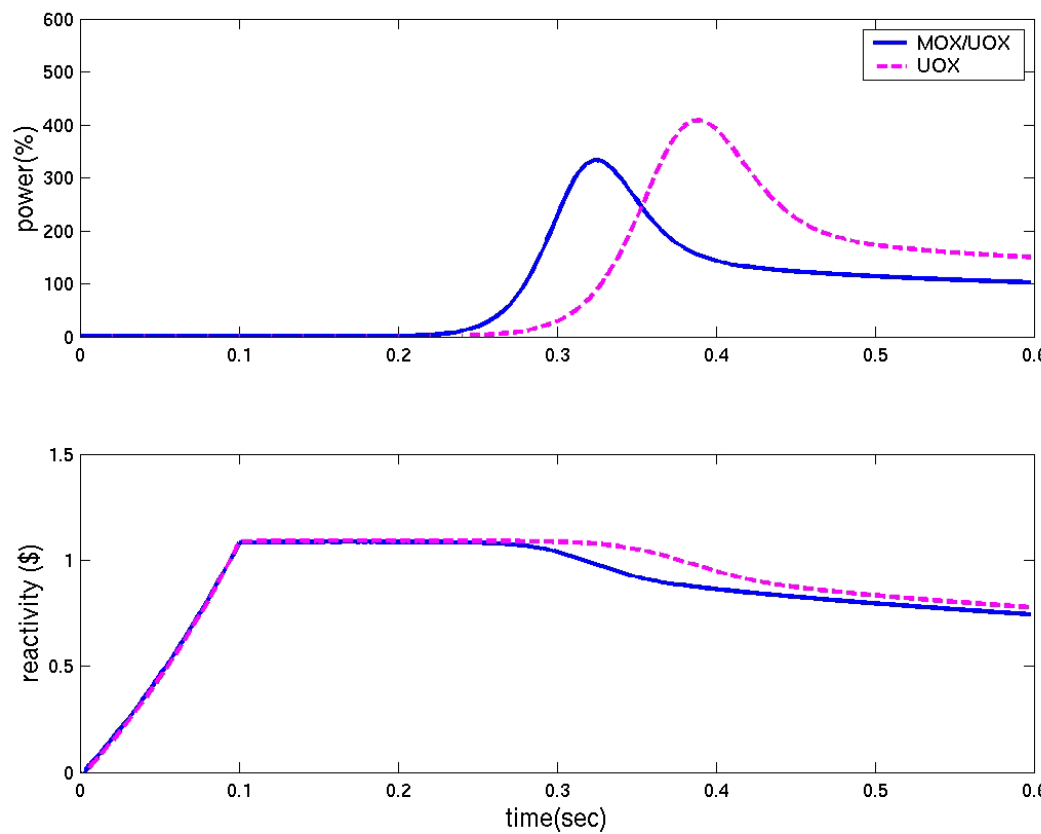
Purdue/NRC OECD Benchmark: MOX Rod Ejection

- Motivation
 - Comparison of multigroup SP3 pin by pin and 2 group, nodal diffusion
 - Comparison of MOX/UOX and UOX core transient response to CEA
- 2-D reactivity insertion problem (Rod Eject from full core)
- Initial HZP conditions, critical boron concentration
- Compare:
 - Eigenvalue
 - Power distribution
 - Critical boron concentration
 - CR worth
 - Transient power, reactivity and fuel temperature

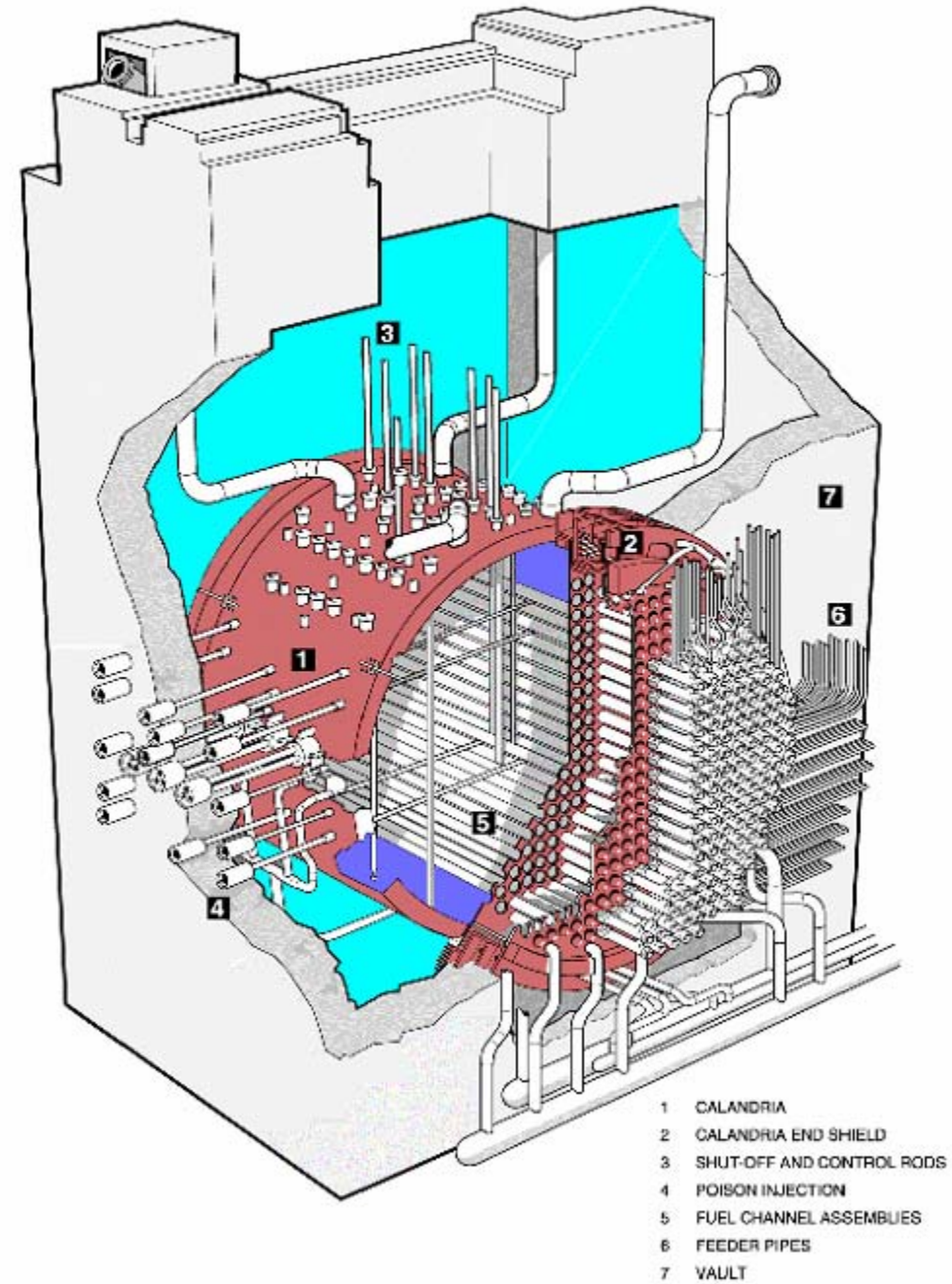
MOX Full Core Design



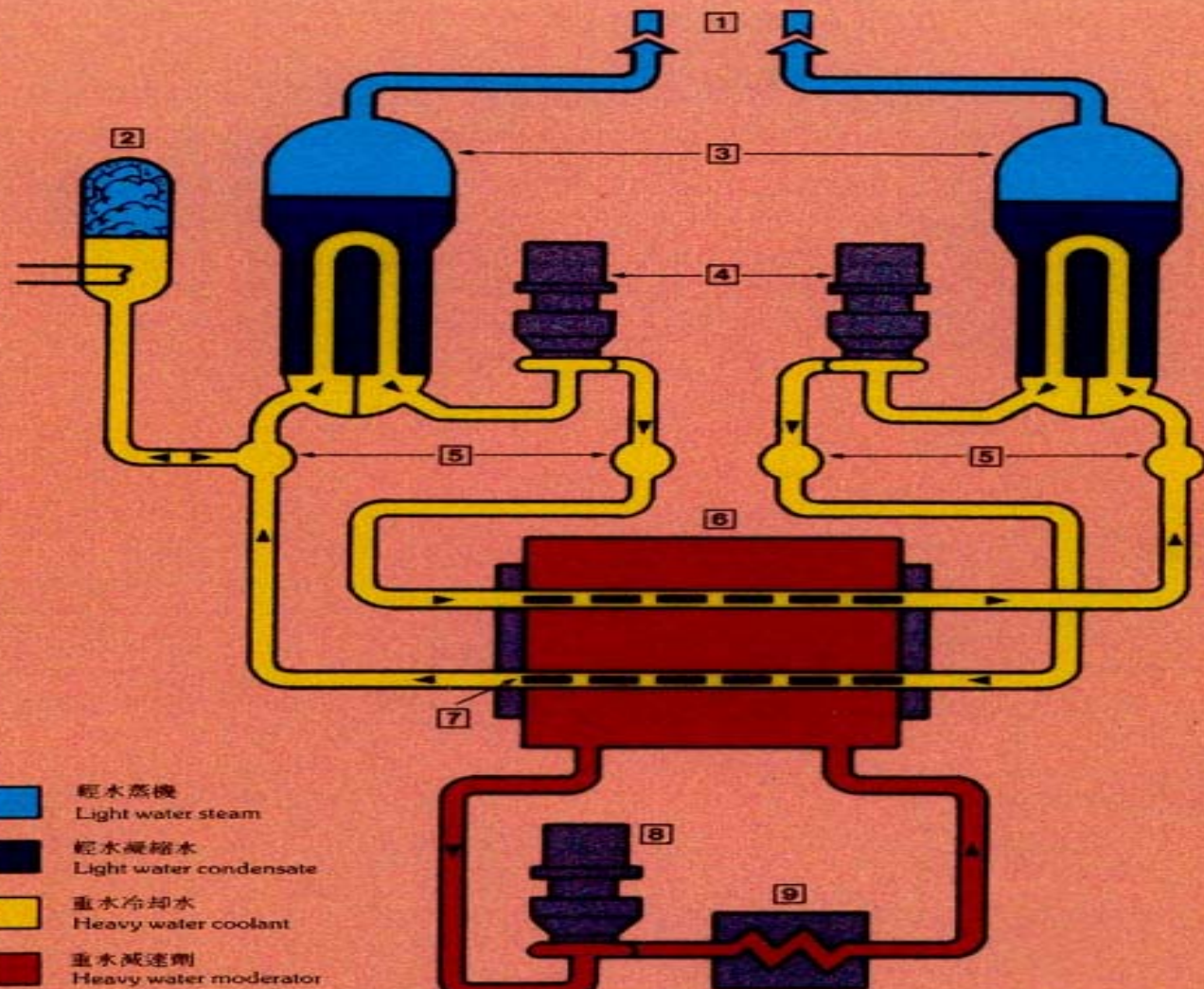
Core Power and Reactivity (MOX/UOX and UOX Cores)



CANDU- PHWR



CANDU Reactor Simplified Flow Diagram



- | | | | |
|-----------|-------------|-------------------------|-----------------------------|
| 1. 主蒸気管 | 6. キャンドリア | 1. Steam pipes | 6. Calandria |
| 2. 加壓器 | 7. 燃料 | 2. Pressurizer | 7. Fuel |
| 3. 蒸氣發生器 | 8. 減速材 ポップ | 3. Steam generators | 8. Moderator pump |
| 4. 冷却材ポンプ | 9. 減速材 熱交換器 | 4. Heat transport pumps | 9. Moderator heat exchanger |
| 5. 冷却材母管 | | 5. Headers | |

Advanced CANDU Reactor

ACR-700

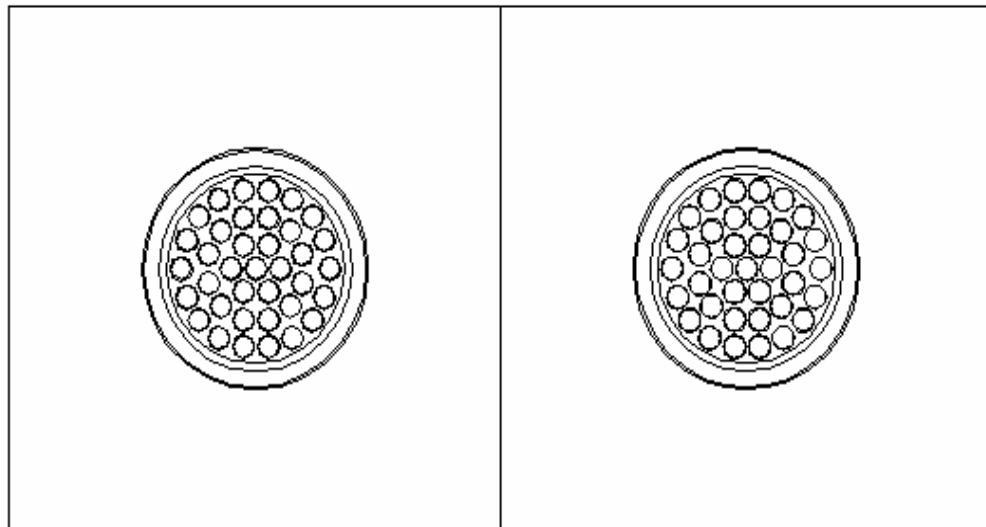
- Modifications:
 - Tighter Pitch Channels
 - Slightly enriched Uranium / Dysprosium BA
 - Replace heavy water coolant with light water
- Is the Void Coefficient Now Negative?

NU CANDU Lattice

Lattice Pitch = 28.58 cm

Fuel Pins = 37

**Moderator Volume
Fuel Volume = 16.4**

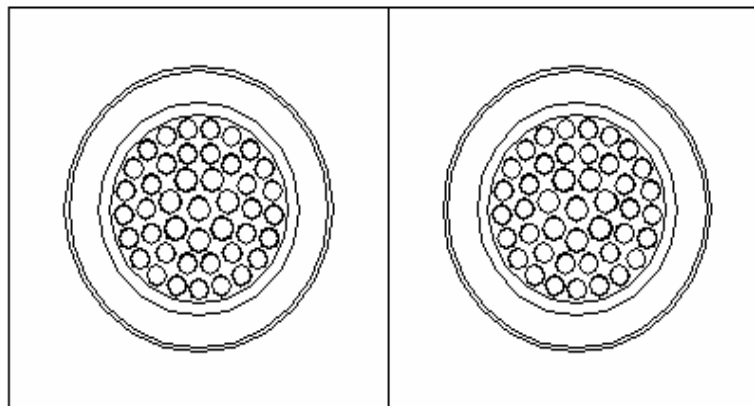


ACR-700

Lattice Pitch = 22.0 cm

Fuel Pins = 43

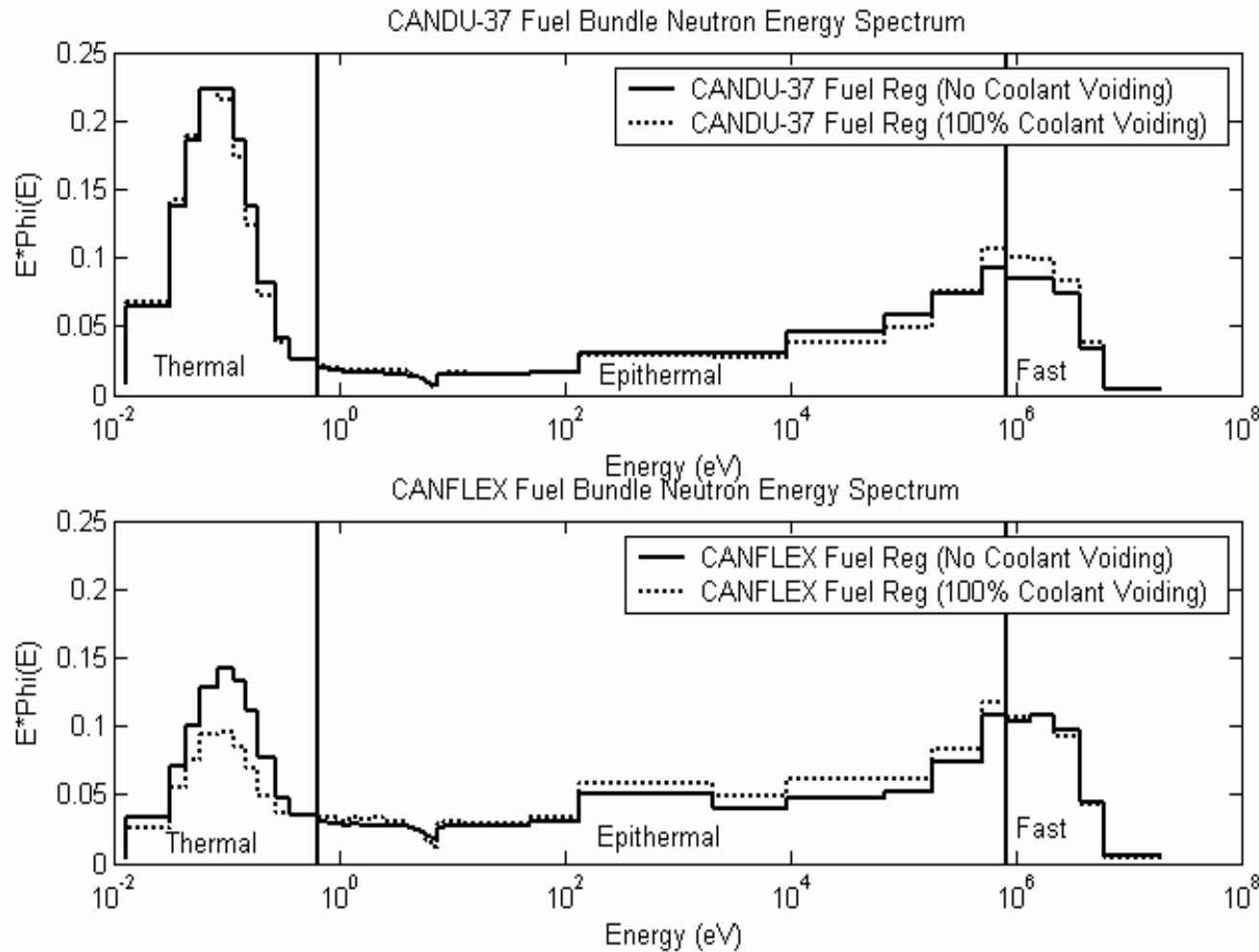
**Moderator Volume
Fuel Volume = 7.1**



CANDU-6 and ACR-700 Fuel Lattices

Effect on CVR of Various Design Changes in the CANDU-6 Lattice

Lattice Pitch	Assembly Type	Fuel Type	BA	CVR	BU	COOLANT
				[mk]	[GWd/t]	
CANDU	37-Element	Natural	No	17.1	0	D2O
CANDU*	CANFLEX	Natural / 2.1% Enriched	No	39.5	0	H2O
ACR-700	CANFLEX	Natural / 2.1% Enriched	No	4.7	0	H2O
ACR-700	CANFLEX	Natural / 2.1% Enriched BA Dy 7.5%	Yes	-1.3	0	H2O
ACR-700	CANFLEX	Natural / 2.1% Enriched BA Dy 7.5%	Yes	-5.6	10	H2O



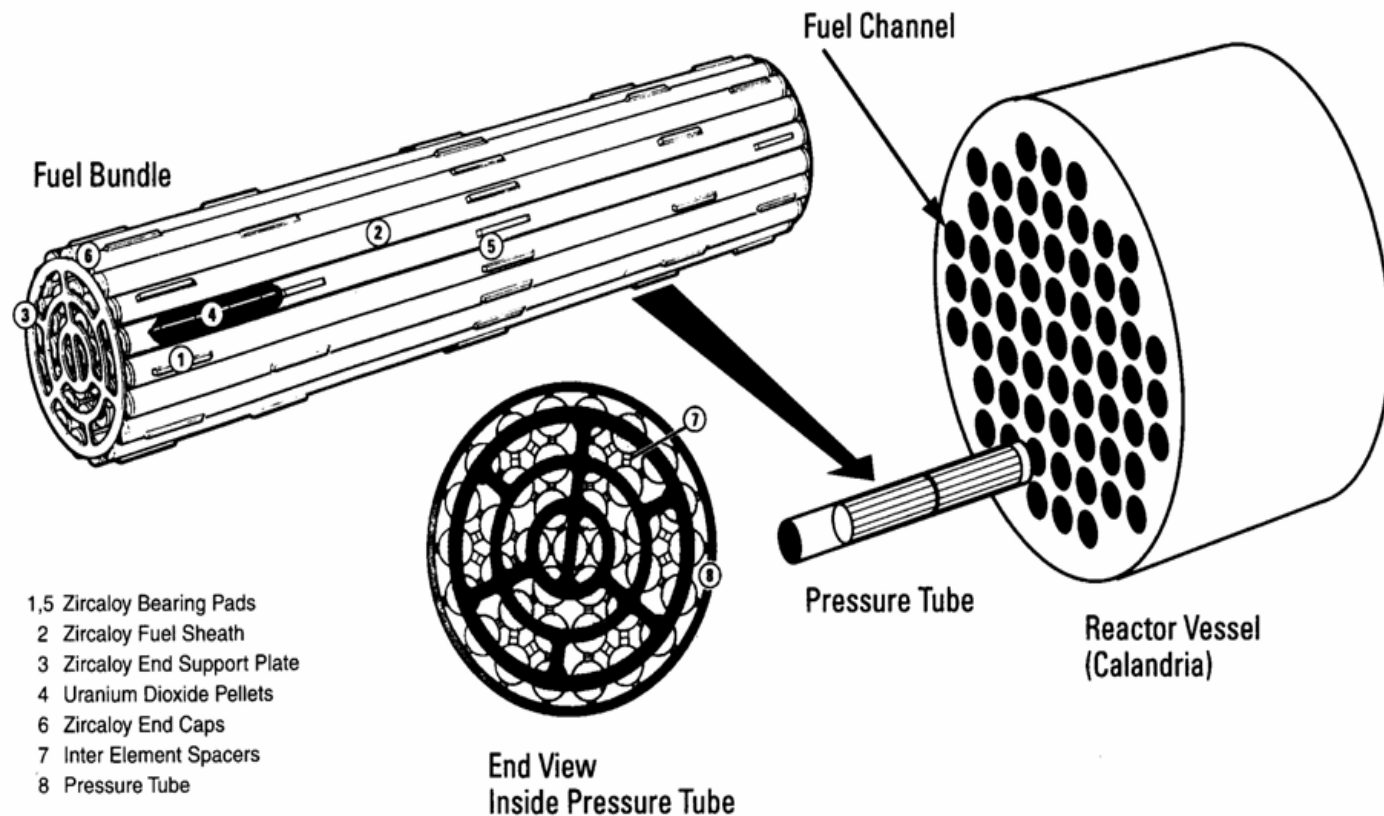
Comparison of Neutron Energy Spectra (0-GWd/t)

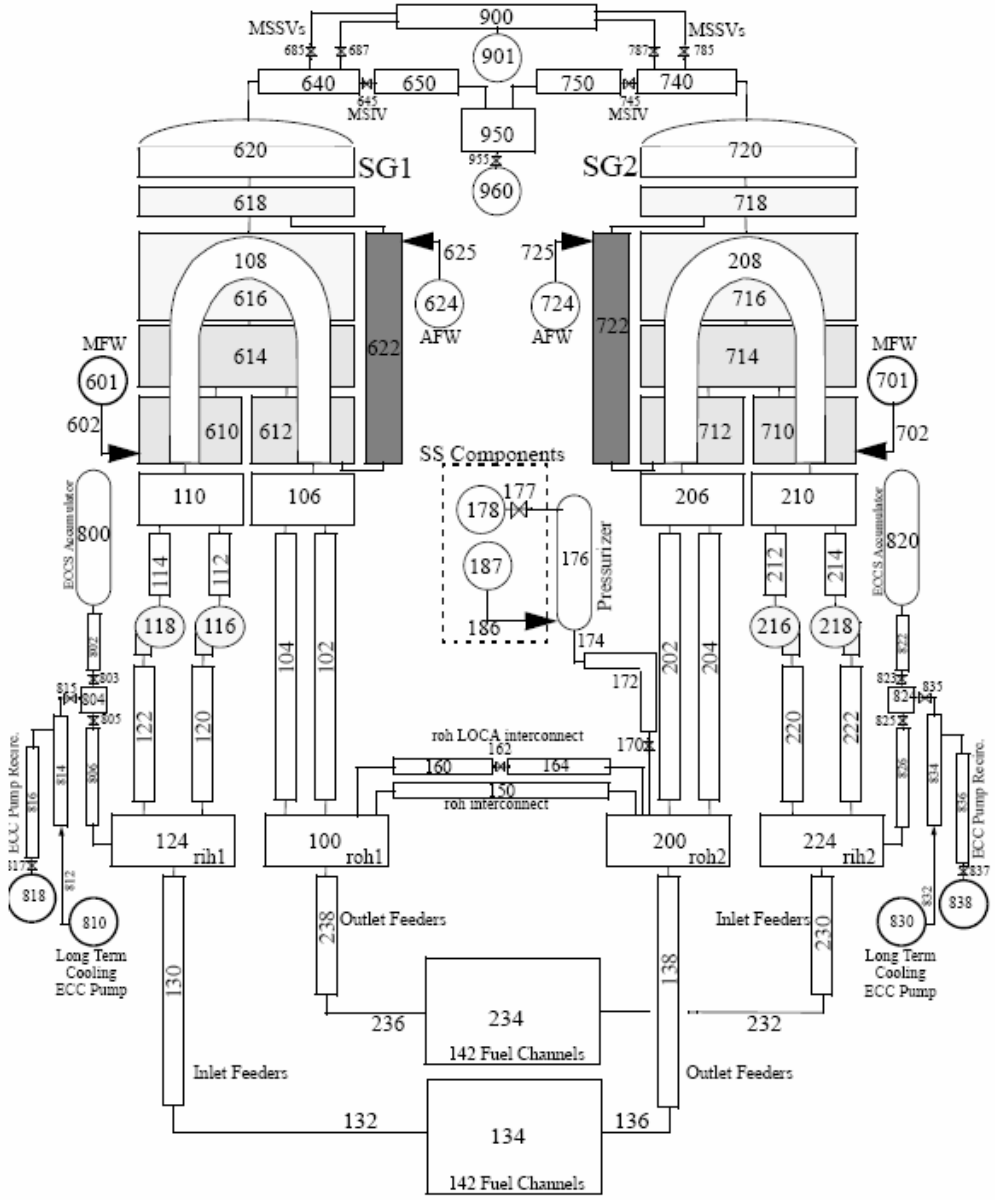
Void Reactivity Components (Fresh Fuel, 0 Gwd/T)

	WIMS AECL*	HELIOS 1.8	
	CANDU-6	CANDU-6	ACR – 700
	[mk]	[mk]	[mk]
$\Delta\eta$	1.8	1.4	-5.2
Δf	3.3	4.3	40
$\Delta\varepsilon$	4.4	4	35.7
ΔpE	9.9	10.2	-68.3
ΔpF	-3.2	-2.4	-3.8
CVR	16.3	17.5	-1.6

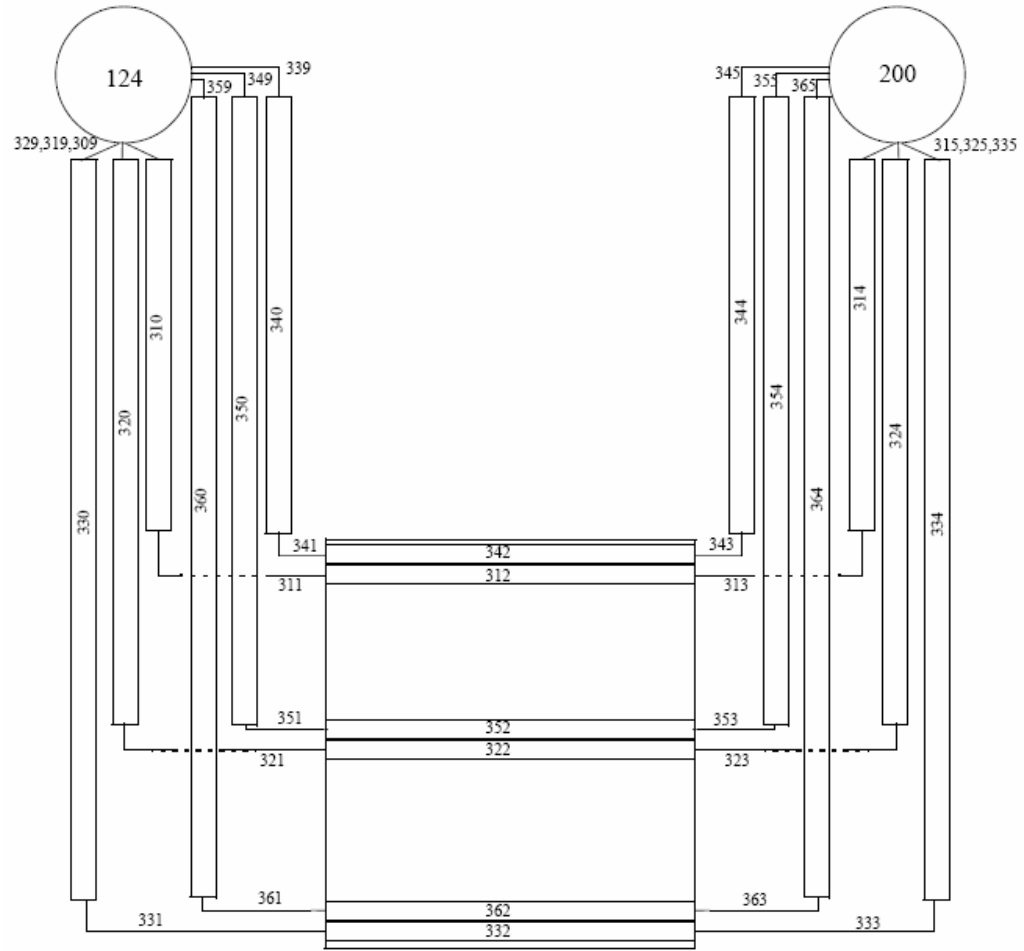
Analysis of Partial Lattice Voiding

Fuel Bundle and Fuel Channel Relationship



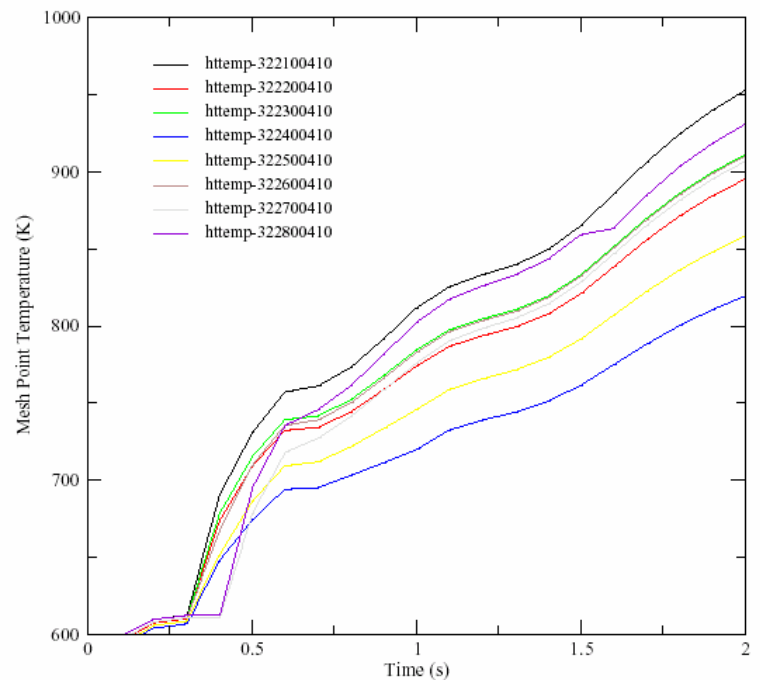
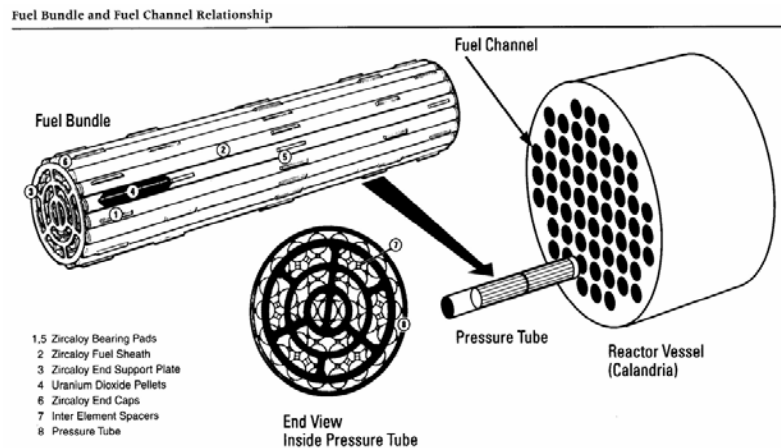


Nodalization Diagram for the Base RELAP5 Model of the ACR-700

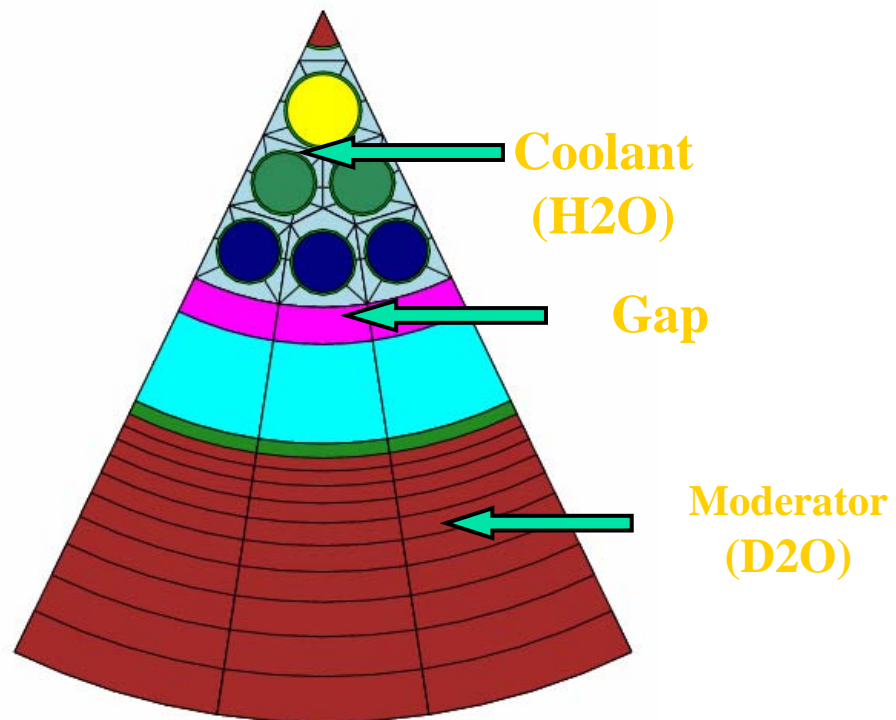


Single Feeders & Fuel Channels Nodalization

Simulation of 25% Inlet Header Break



1/7th Symmetric HELIOS Model of CANFLEX Assembly



$\Delta\rho$ vs. Homogeneous Coolant Density Reduction / Fractional Coolant Reduction

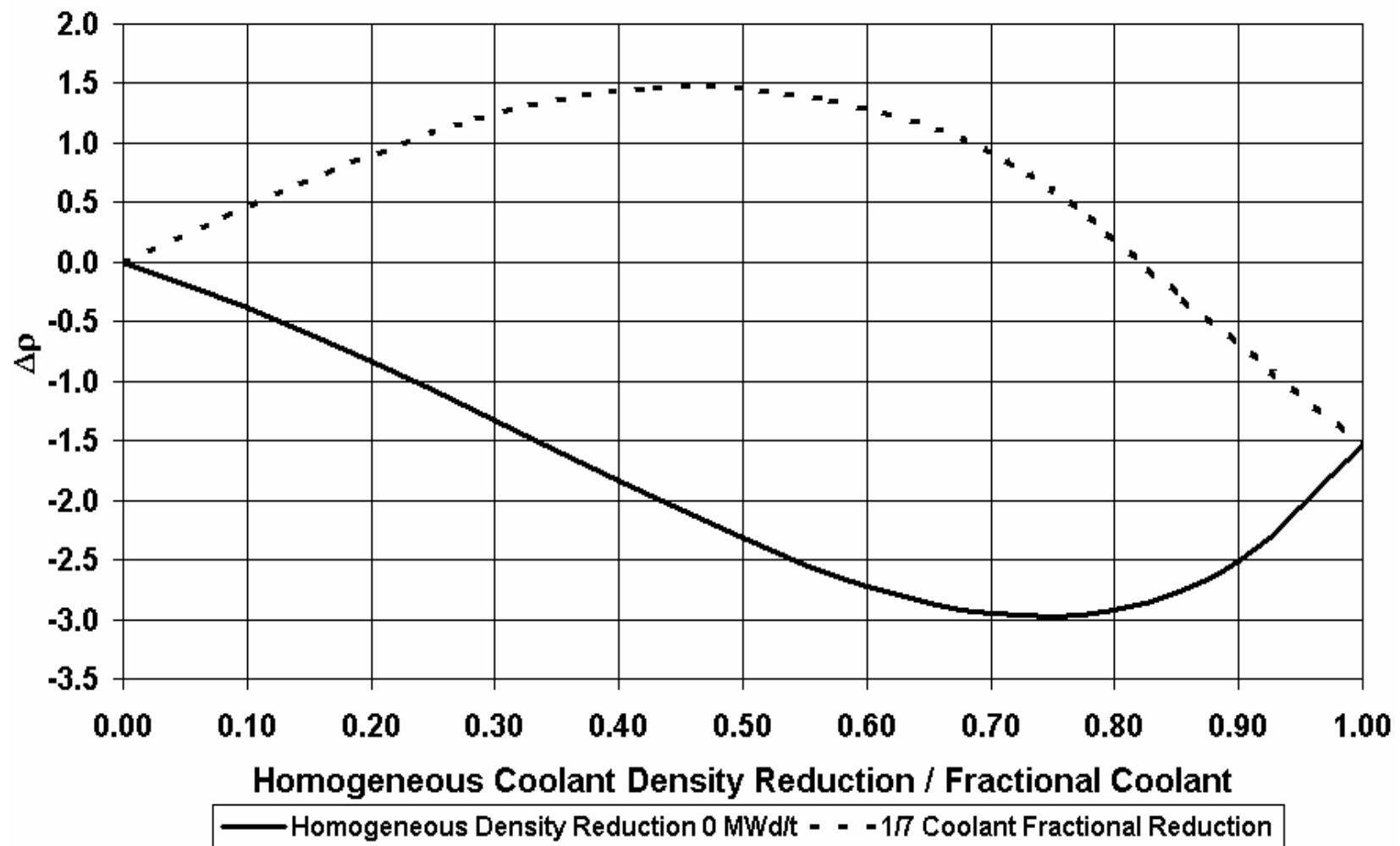


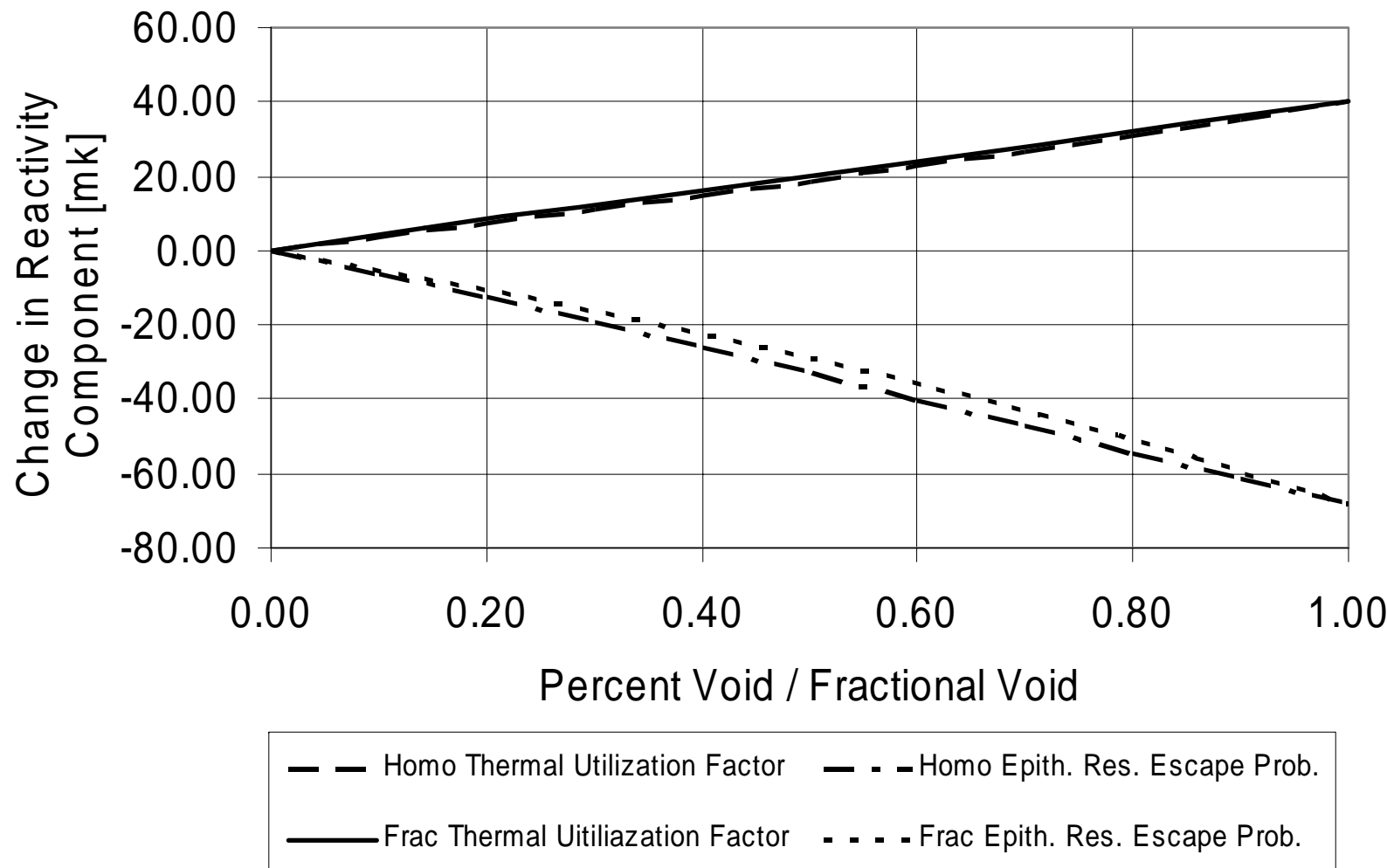
Table 3 Reactivity Components for Homogeneous Reduction in Coolant Reactivity

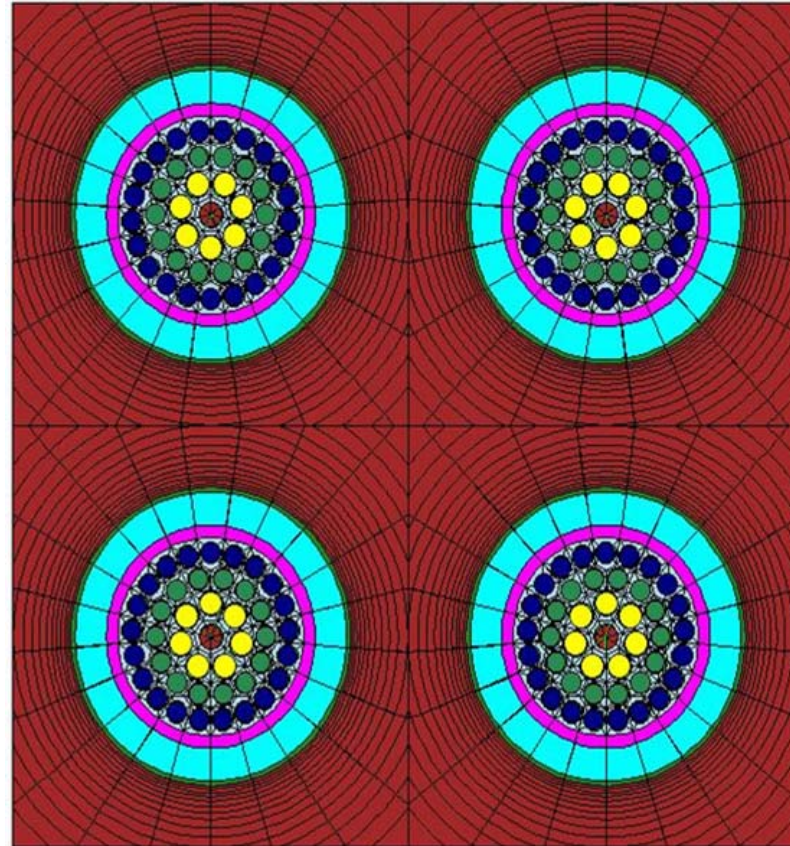
Void Fraction ->	0.1	0.2	0.3	0.4	0.5	0.6	0.7	0.8	0.9	1
$\Delta\eta$	-0.3	-0.6	-0.9	-1.3	-1.7	-2.3	-2.8	-3.5	-4.3	-5.2
Δf	3.6	7.3	11	14.9	18.7	22.7	26.8	31	35.4	40
$\Delta\epsilon$	2.8	5.7	8.8	12	15.4	19.1	22.8	26.9	31.2	35.7
Δp_E	-6.2	-12.6	-19	-26.1	-33.1	-40.2	-47.6	-54.5	-61.5	-68.3
Δp_F	-0.2	-0.5	-0.9	-1.3	-1.5	-2	-2.8	-2.7	-3.2	-3.8
Sum	-0.3	-0.8	-1.3	-1.8	-2.2	-2.7	-3.6	-2.9	-2.5	-1.7

Table 4 Reactivity Components for Heterogeneous Reduction in Coolant Reactivity

Fraction Of Lattice ->	1/7	2/7	3/7	4/7	5/7	6/7	1
$\Delta\eta$	-1.1	-2	-2.7	-3.4	-4.2	-4.8	-5.2
Δf	6	11.7	17	22.8	28.6	34.4	40
$\Delta\varepsilon$	3.9	8.2	13	17.6	23.1	29.1	35.7
Δp_E	-7.8	-15.7	-24	-33.7	-44.1	-55.9	-68.3
Δp_F	-0.5	-1	-1.5	-2	-2.6	-3.2	-3.8
Sum	0.7	1.3	1.5	1.3	0.8	-0.4	-1.6

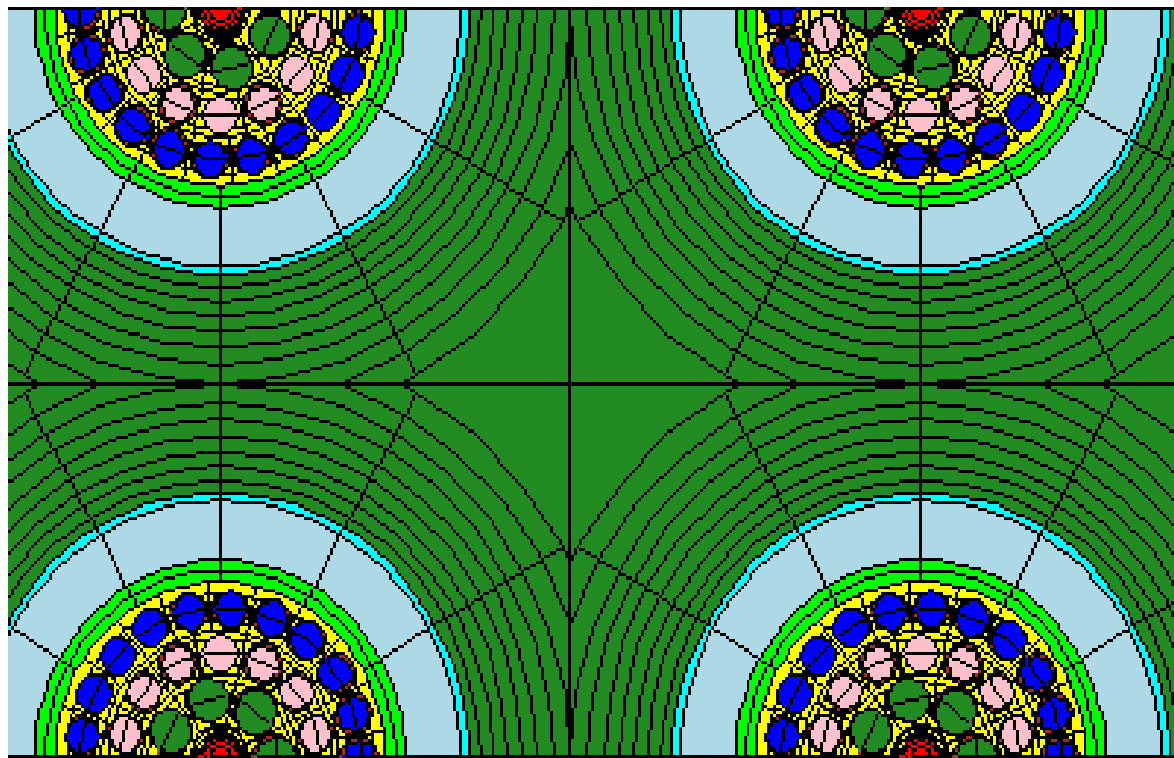
Reactivity Change Components vs. Percent Void / Fractional Void





HELIOS 2x2 Lattice Physics Model

HELIOS 2x2 Model Used for CNSC Calculations



Comparison of Purdue and CNSC 2x2 HELIOS Results

	keff			CVR (mk)	
	Cooled	CB-Voided	Full-Voided	CB	Full-Voided
				Voided	
Purdue Model	1.25378	1.26007	1.2526	3.5	-2.1
CNSC Model	1.25356	1.25878	1.25052	3.3	-1.9

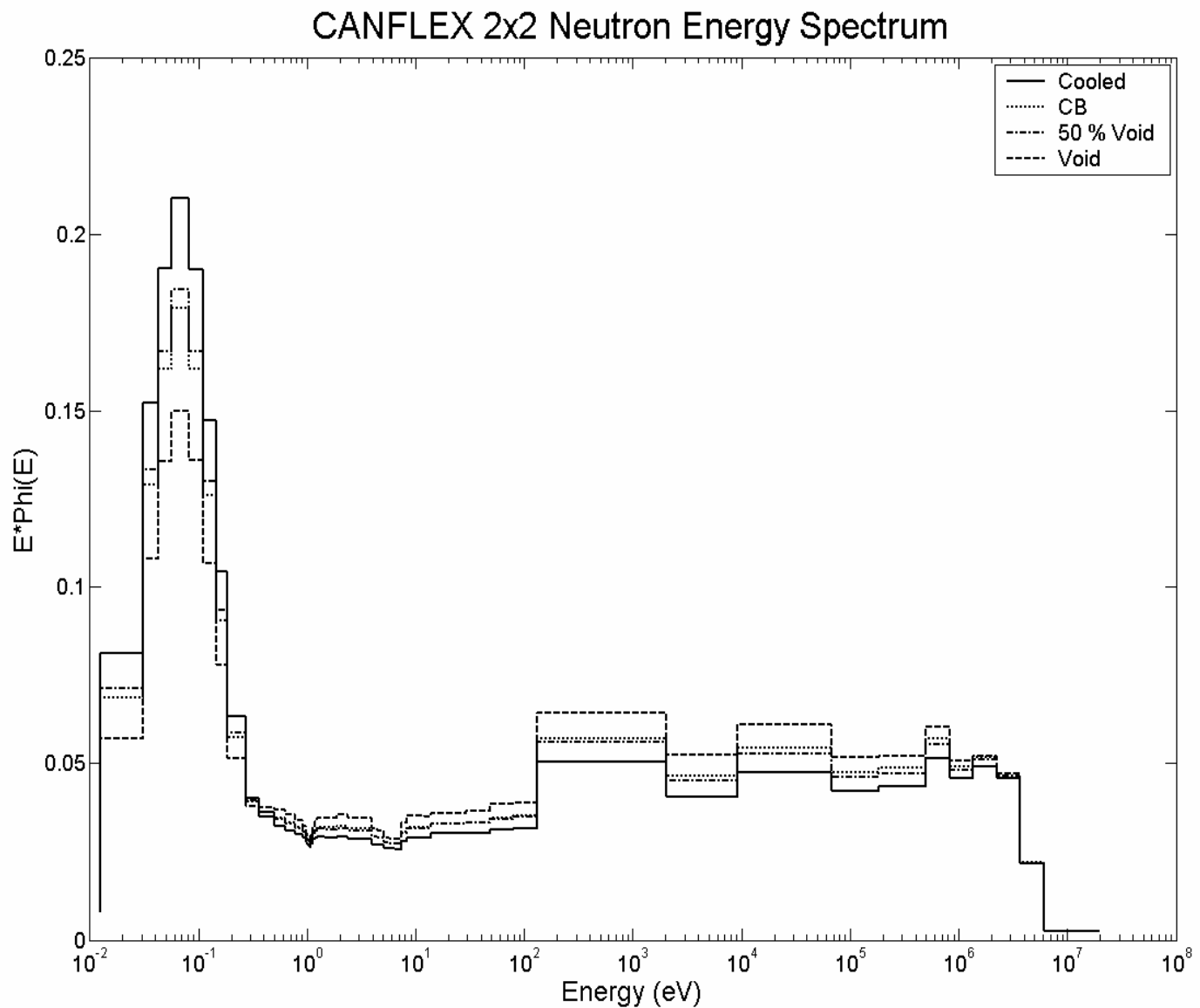


Fig. 9. Neutron Energy Spectrum for 2x2

Analysis of CVR

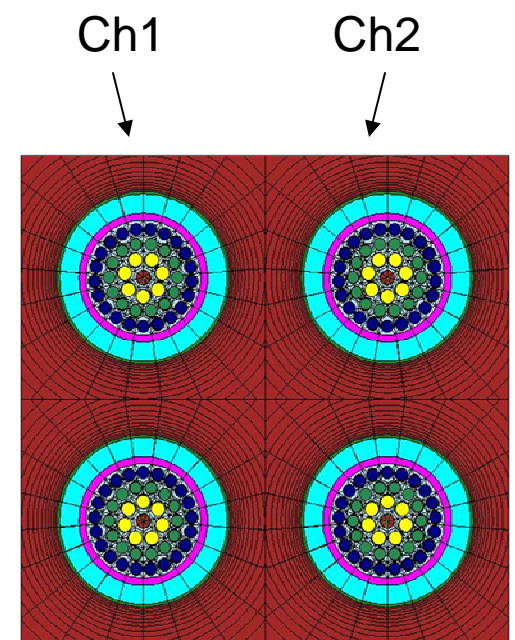
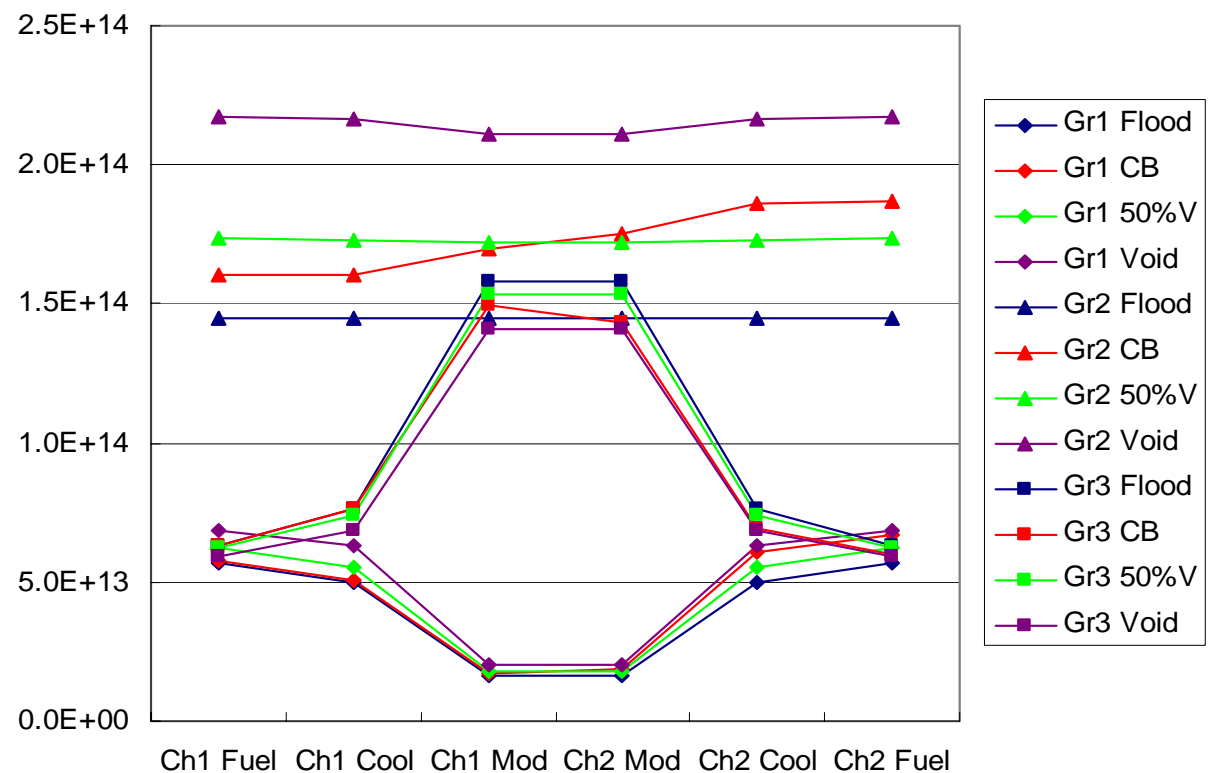
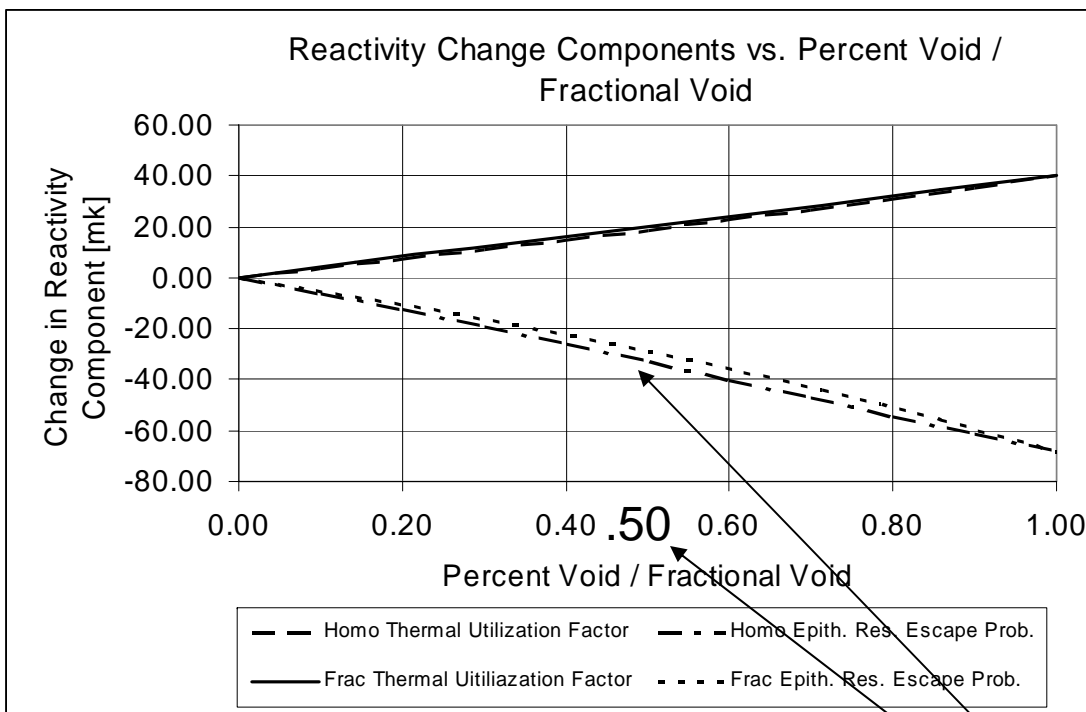


Figure 10 Spatial Distribution of Fluxes in 2x2 Channels

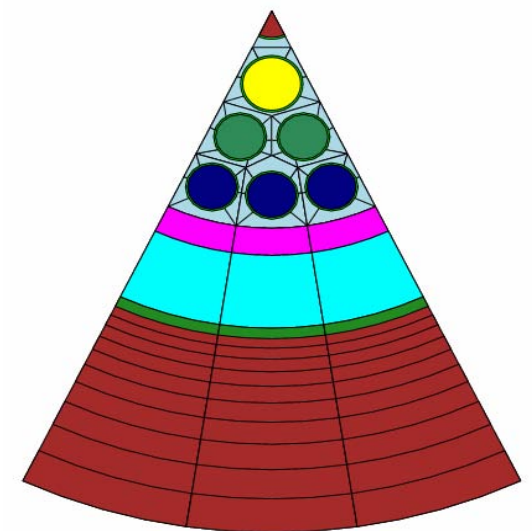
Table 12 Comparison of Four Factors for Checkerboard and Homogeneous Voided States

	50% Homogeneous Void	Checkerboard	Fully Voided
$\Delta\eta$	-1.8	-3.1	-5.2
Δf	18.7	20.7	39.9
$\Delta\varepsilon$	15.4	14.6	35.7
Δp_E	-33.2	-26.6	-68.5
Δp_F	-1.7	-2.0	-4.0
Sum	-2.5	+3.5	-2.1

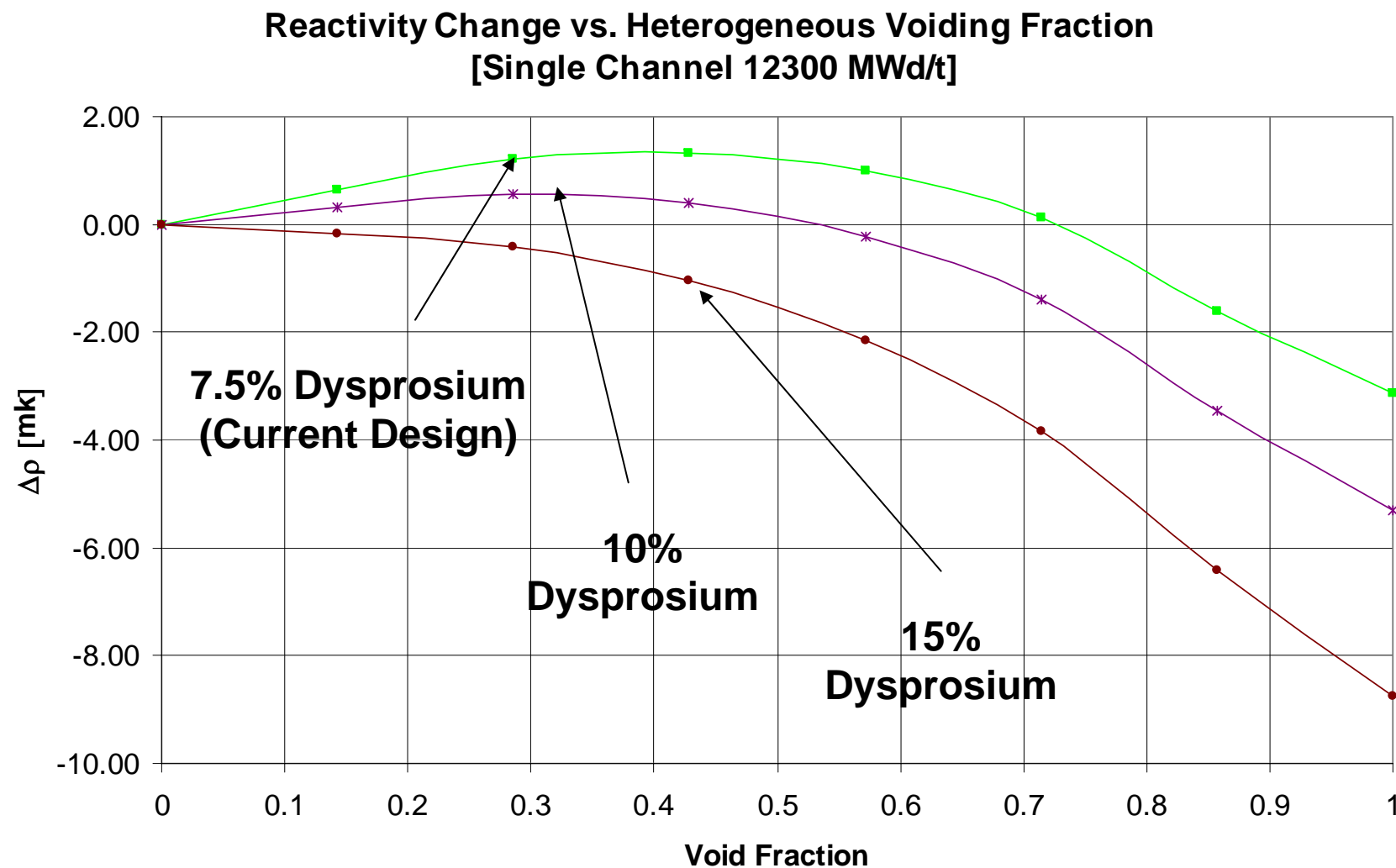
Single Assembly Checkerboard Analysis



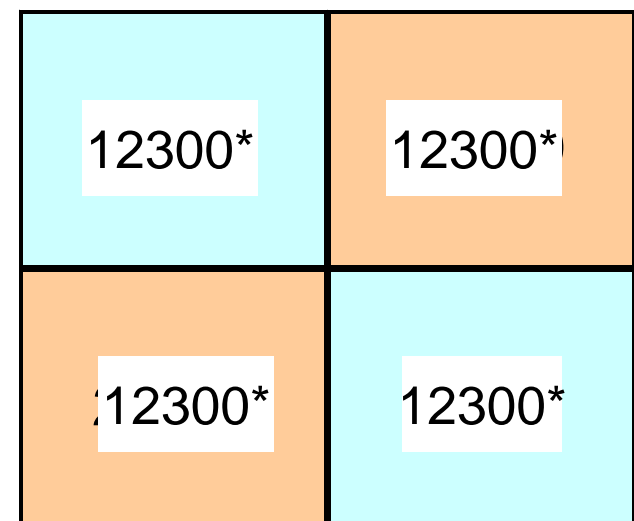
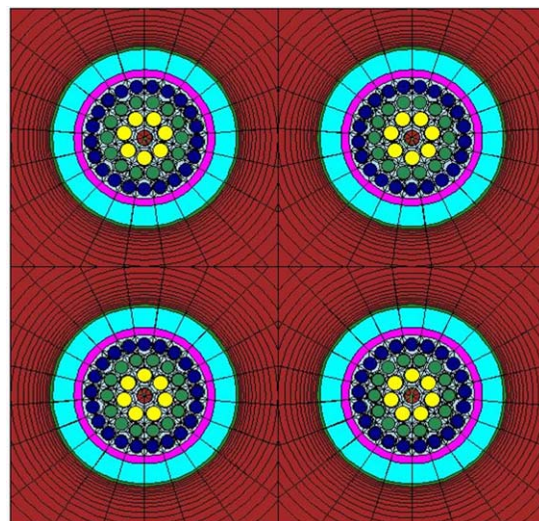
50%
Reduction in Coolant



Preliminary Analysis of Design Options to Achieve Negative CVR w/ Checkerboard Voiding



HELIOS vrs PARCS/HELIOS



Burnup Distribution (MWD/MT)* for 2x2 Homogeneous Analysis

Results for 2x2 Heterogeneous Burnup Case

		Cooled	CB1-Voided	CB2-Voided	Full-Voided	CB1-Voided	CB2-Voided	Full-Voided
HELIOS (47-G)	Periodic	1.03505	1.03719	1.04205	1.0314	2	6.5	-3.4
PARCS w/o ADFs (2-G)	Periodic	1.03846	1.03715	1.04421	1.03544	-1.2	5.3	-2.8
HELIOS -PARCS (pcm)	Periodic	-320	213	-316	-364			

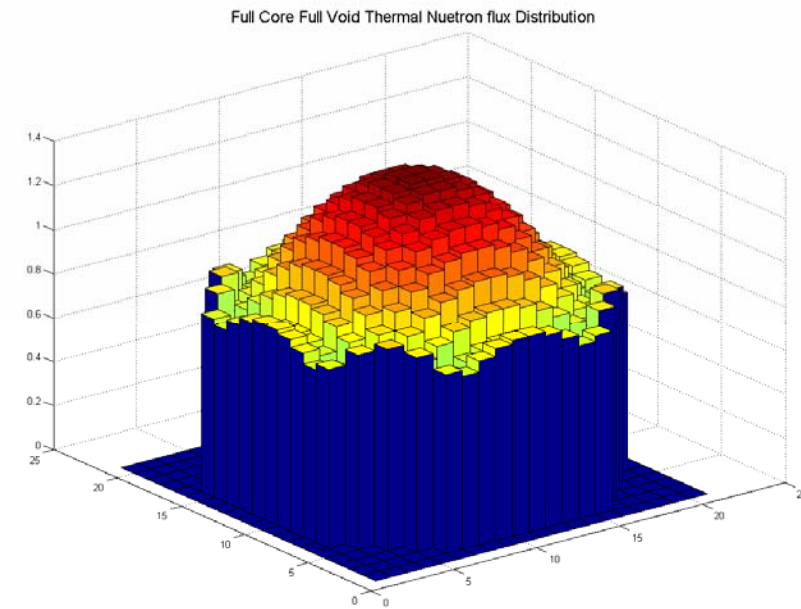
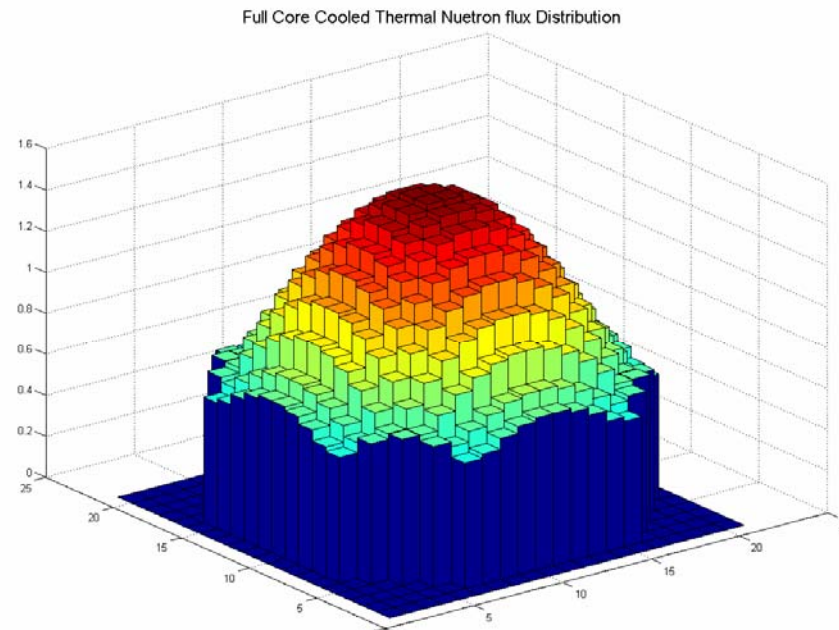
Results for 2x2 Heterogeneous Burnup Case: PARCS with HELIOS “Colorset” Cross Sections (w/o ADFs)

	B.C	k_{eff}				CVR (mk)		
		Cooled	CB1-Voided	CB2-Voided	Full-Voided	CB1-Voided	CB2-Voided	Full-Voided
PARCS (2-G) w/o ADFs	Periodic	1.03418	1.03628	1.04196	1.03053	2.0	7.2	-3.4
HELIOS (47-G)	Periodic	1.03505	1.03719	1.04205	1.03140	2.0	6.5	-3.4
HELIOS- PARCS (pcm)	Periodic	87	91	9	87			

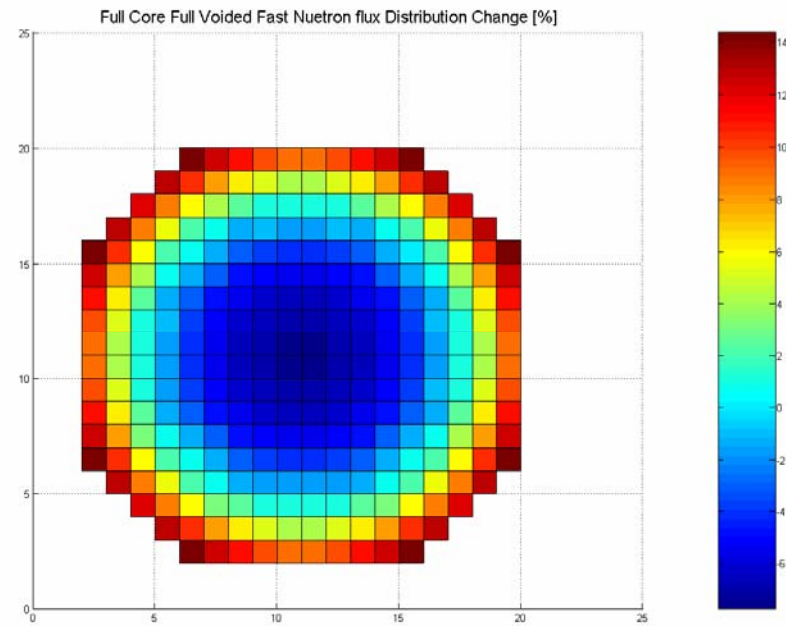
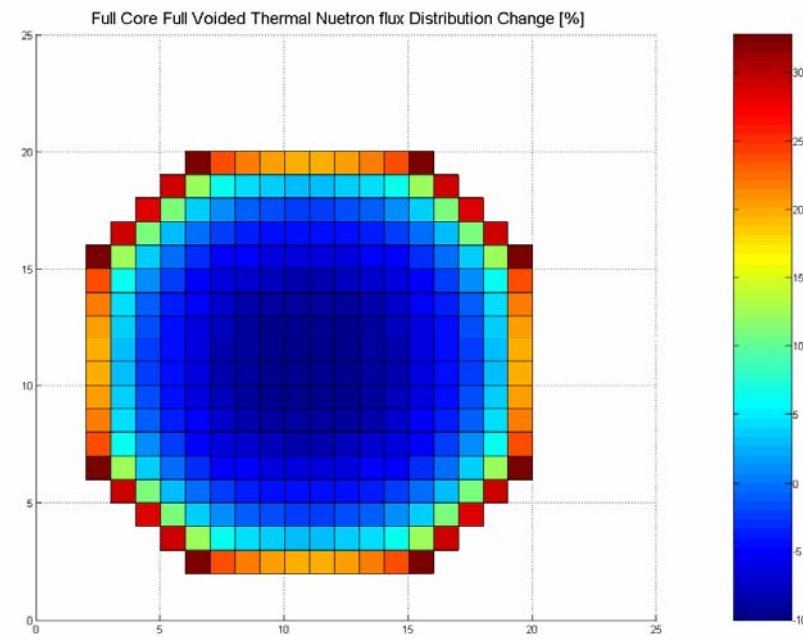
Comparison of PARCS Multigroup Calculations with HELIOS (w/o ADFs)

	B.C	keff				CVR (mk)		
		Cooled	CB1-Voided	CB2-Voided	Full-Voided	CB1-Voided	CB2-Voided	Full-Voided
PARCS (2-G)	Periodic	1.03846	1.03715	1.04421	1.03544	-1.2	5.3	-2.8
PARCS (4-G)	Periodic	1.03730	1.03545	1.04399	1.03409	-1.7	6.1	-3.0
PARCS (8-G)	Periodic	1.03739	1.03870	1.04291	1.03447	1.2	5.1	-2.7
PARCS (47-G)	Periodic	1.03690	1.03781	1.04269	1.03398	.8	5.4	-2.7
HELIOS (47-G)	Periodic	1.03505	1.03719	1.04205	1.03140	2.0	6.5	-3.4

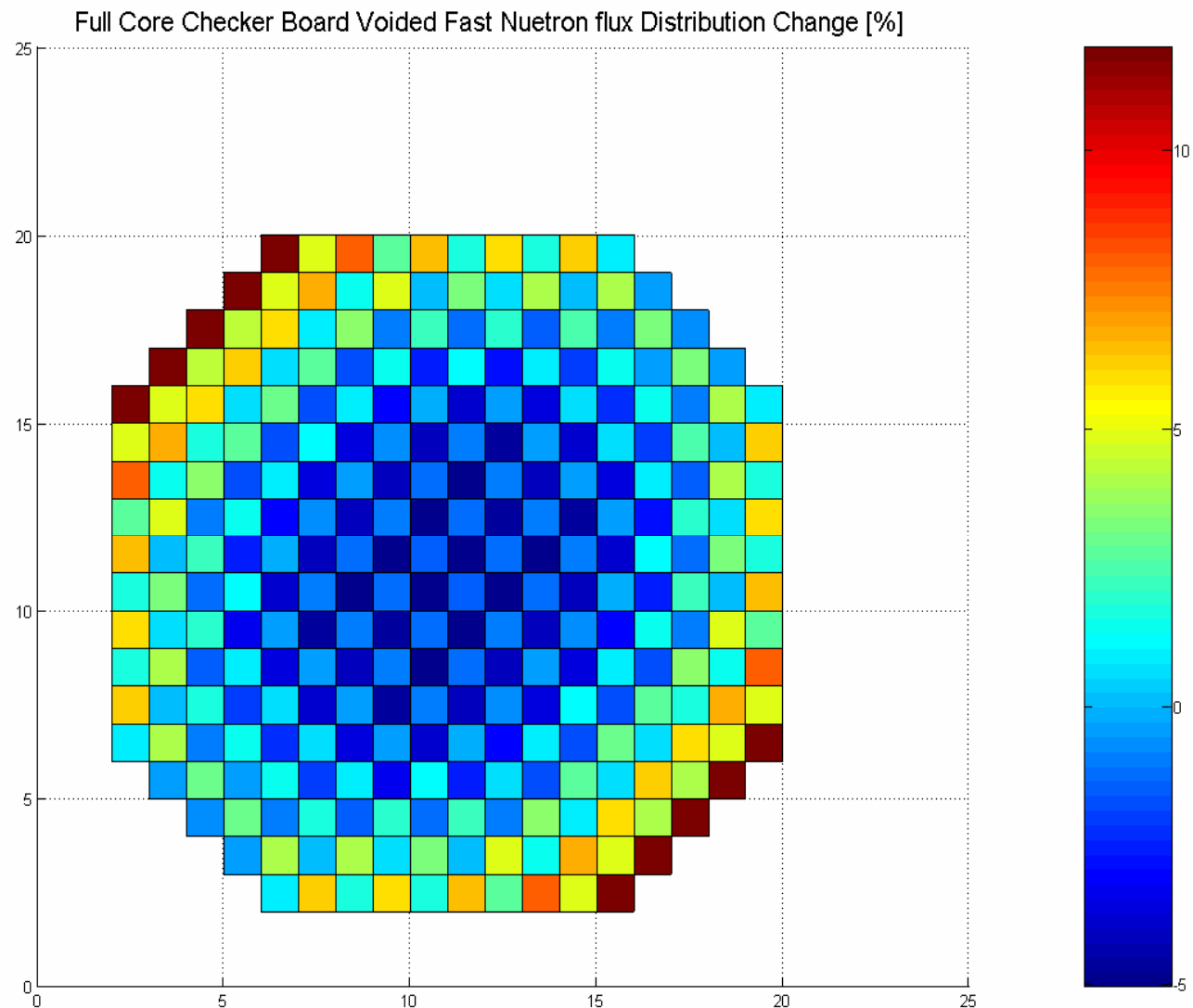
ACR-700 3-D, Full Core Model



Thermal Flux Distributions Before and After Core Voiding



Change in Thermal and Fast Flux Distributions for Uniform Core



Change in Fast Flux upon Checkerboard Voiding

Summary of Results for 3D PARCS Core Calculation (Homogeneous Burnup Distribution)

	Radial	Axial	keff			CVR (mk)	
	B.C.	B.C.	Cooled	CB-Voided	Full-Voided	CB-Voided	Full-Voided
PARCSFull Core (3-D)	Zero Incoming Current	Zero Incoming Current	1.16551	1.16715	1.16012	1.2	-4.0
PARCSFull Core (2-D)	Zero Incoming Current	Reflective	1.17202	1.17478	1.16911	2.0	-2.1
PARCS 2x2 (2-G)	Periodic		1.19005	1.19425	1.18963	3.0	-0.3

PARCS Results for Full Core Checkerboard Voided Configurations

	Radial B.C.	Axial B.C.	Keff				CVR (mk)		
			Cooled	CB-1 Voided	CB-2 Voided	Full- Voided	CB-1 Voided	CB-2 Voided	Full- Voided
2-D	Zero Incoming Current	Reflectiv e	1.01911	1.02039	1.02575	1.01389	1.2	6.3	-5.1
3-D	Zero Incoming Current	Zero Incoming Current	1.01335	1.01361	1.01909	1.00598	0.3	5.6	-7.2*

*Compares w/ Other FULL CORE VOIDED Results:

AECL, Oct PIRT Mtg: CVR = -7.0mk

CNSC, MCNP: CVR = -6.5mk

PARCS Modifications for ACR-700

- Methods Modifications
 - The Multigroup, SP3 Kernel developed as part of the PARCS MOX LWR work will be directly applicable to the ACR-700
 - Additional Methods work will only be required in the area of Homogenization and Dehomogenization
 - Homogenization
 - “Zero Current” Lattice cross sections are not sufficient to describe accurately the heterogeneous burnup or checkerboard voided conditions
 - Alternative Methods
 - Pretabulated “albedos” which treat the lattice boundary condition as an additional “feedback” variable (Clarno, Adams 2004)
 - Explicitly model “moderator” and “fuel/coolant” regions
 - Dehomogenization
 - Minor additional upgrades to the existing pin power reconstruction methods in PARCS because of the irregular CANFLEX bundle geometry

Summary/Conclusions

- U.S. NRC
 - Reactor Physics Methods Development
 - Coupled Neutronics/Thermal-Hydraulic Code Development for Reactor Transient Simulation
- U.S. DOE
 - Fuel Cycle Development and Analysis for Advanced Reactor Concepts (NERI: 2000-2003)
 - Coupled CFD/MOC (INERI)
 - Numerical Methods (NEER)

DOE I-NERI

**The Numerical Nuclear Reactor for High-Fidelity
Integrated Simulation of Neutronic, Thermal-
Hydraulic, and Thermo-Mechanical Phenomena**

David P. Weber

Argonne National Laboratory

Han Gyu Joo

Korea Atomic Energy Research Institute

Thomas J. Downar

Purdue University

Chang Hyo Kim

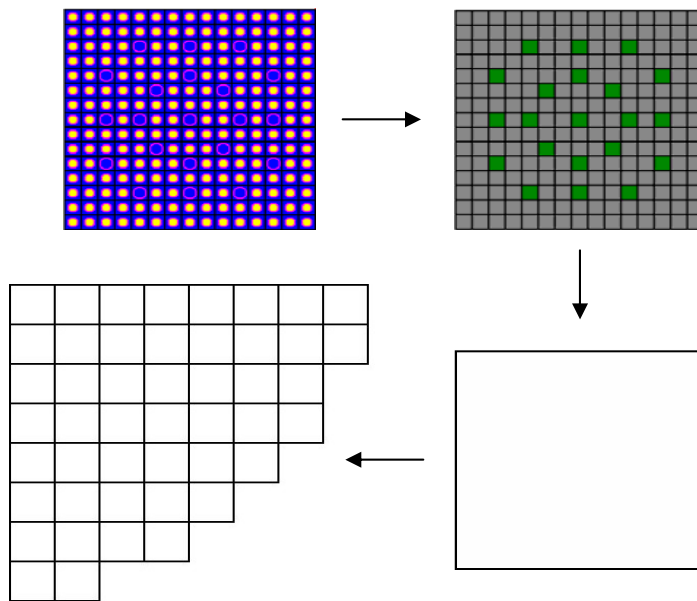
Seoul National University

Project Goal and Objectives

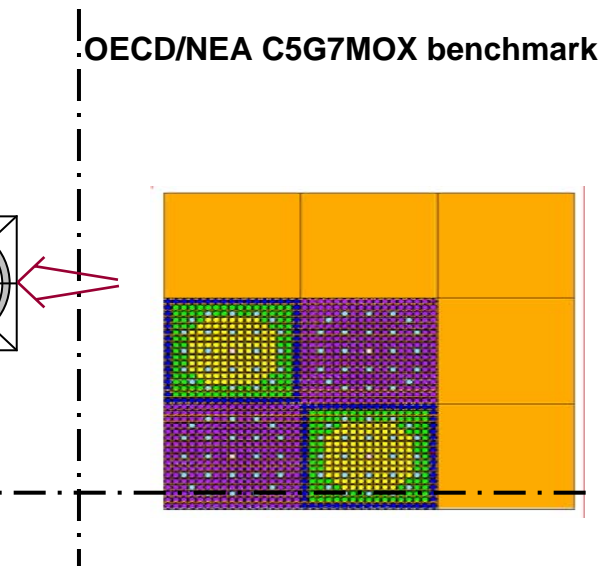
- Goal
 - Develop a *Numerical Nuclear Reactor* which Performs High-Fidelity, Integrated Simulation of the Multi-Physics Phenomena Occurring in Light Water Reactors
(Multi-Physics Phenomena = Neutronics, Thermal-Hydraulic(T-H), and Thermo- Mechanical Phenomena which are Mutually Coupled)
- Objectives
 - Develop a 3-D Whole-Core Neutron Transport Code that Can Perform Core Calculations keeping the Sub-Pin Level Details
 - Employ Mechanistic and Detailed Computational Fluid Dynamics (CFD) Solutions for T-H Analysis
 - Incorporate Structural Change using FEM Based Thermo-Mechanical Solutions
 - Couple the Neutronics/CFD/Mechanical Modules Employing an Efficient Coupling Scheme

Numerical Reactor Neutronics Concept

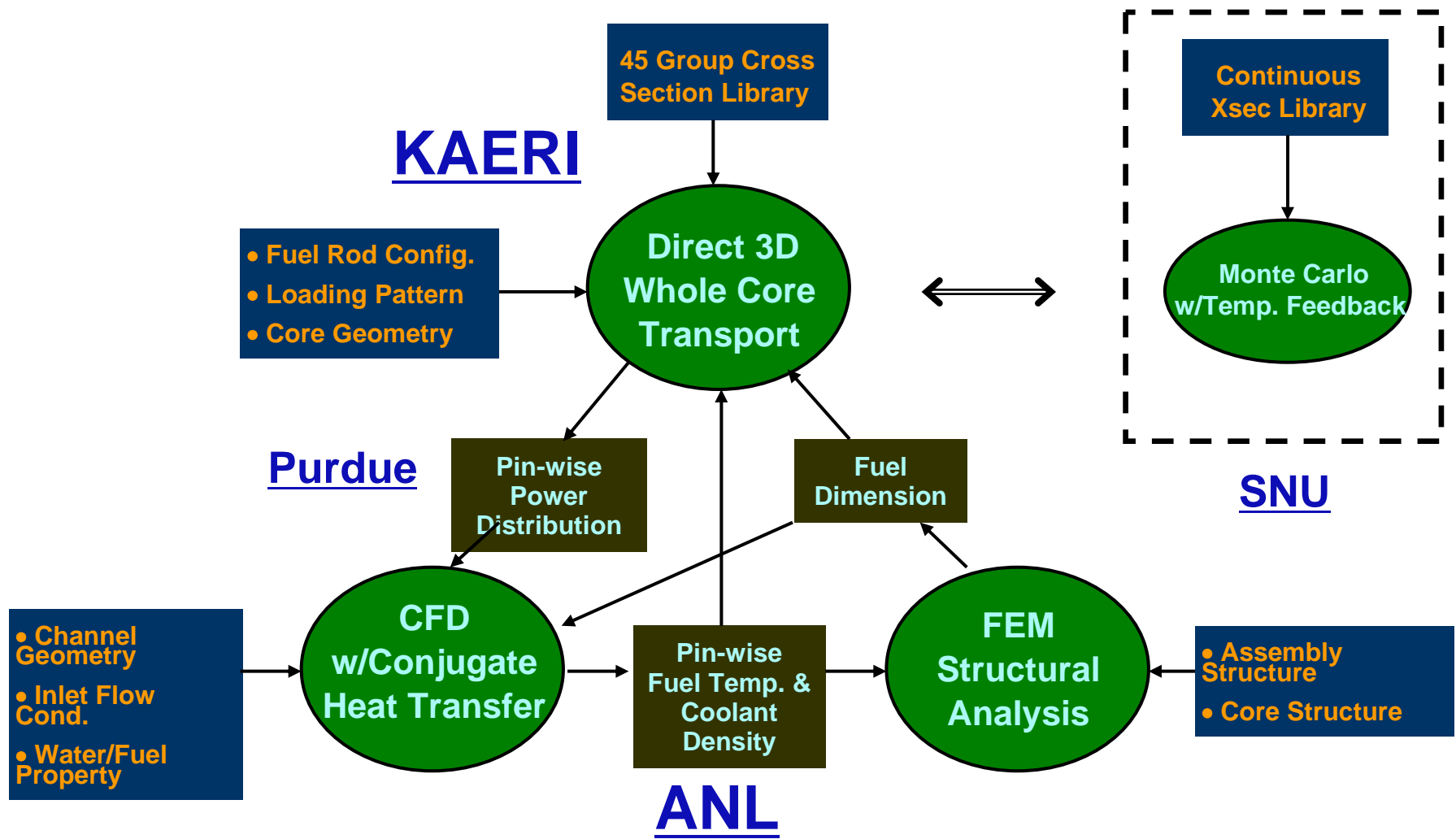
- Conventional Approach
 - Multi-step calculations involving homogenization and group condensation
 - Diffusion approximation for core calculation



- Numerical Reactor
 - Direct whole core transport calculation with explicit representation of local heterogeneity
 - Pin-wise T/H feedback through coupling with CFD

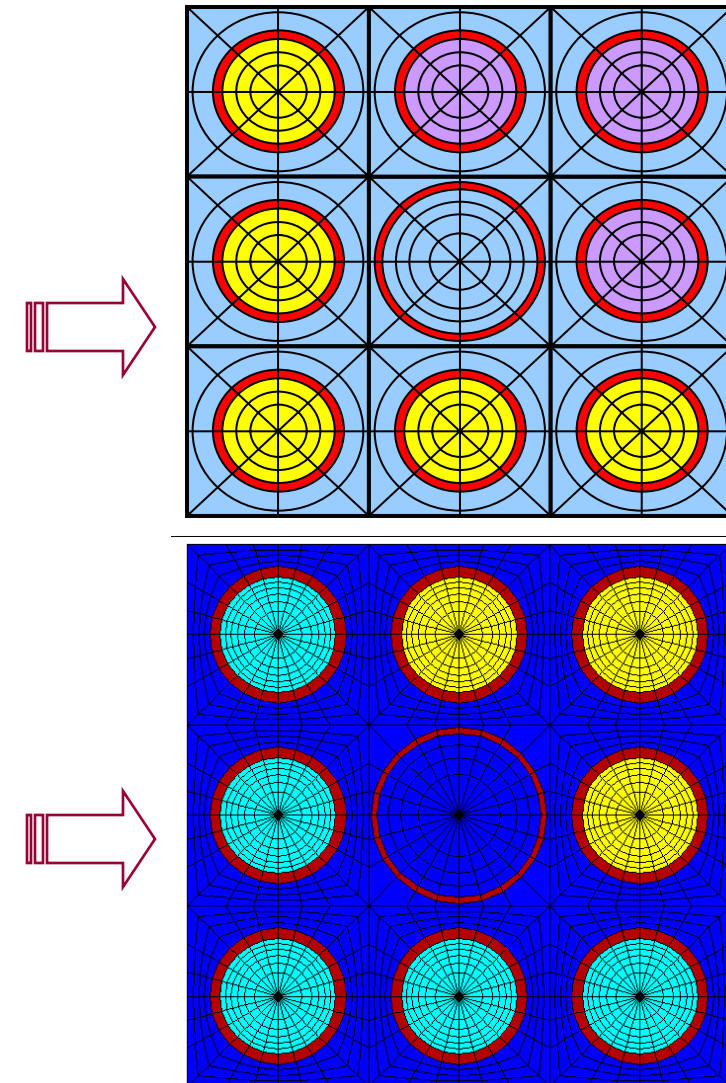


Numerical Reactor Elements and Participants

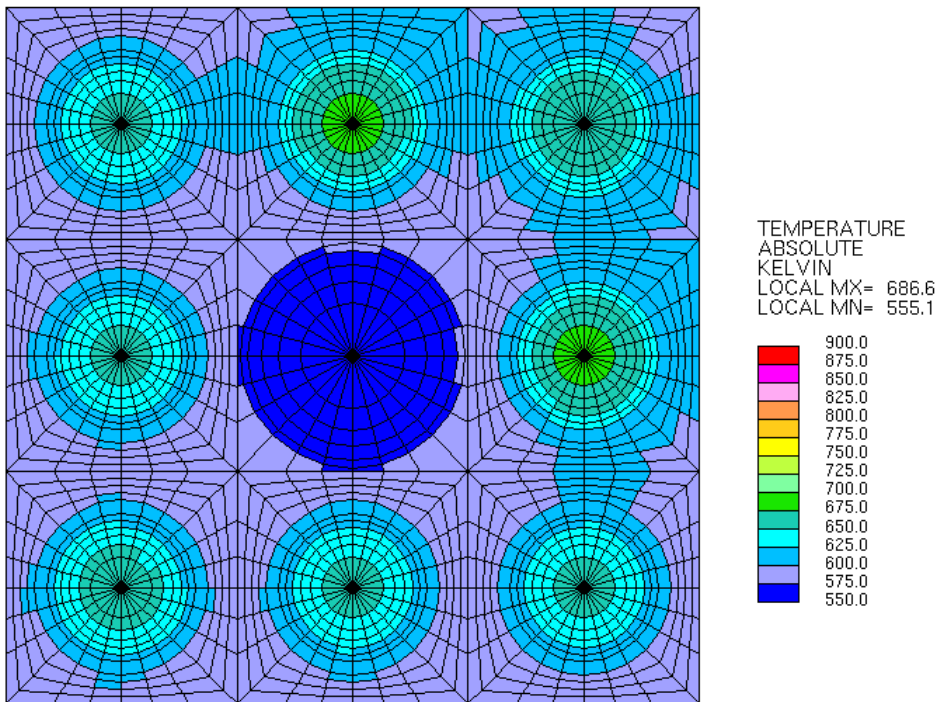


Test Problem I: 3x3 Model

- Configuration:
 - 3 MOX pins, 5 UO₂ pins and a central guide tube
- DeCART discretization:
 - 12 axial planes
 - 9 pins
 - 6 rings / pin
 - 8 azimuthal regions / pin
 - ~5 thousand mesh
- STAR-CD discretization:
 - Radial:
 - Fuel: 6 rings inside fuel, 1 clad ring, 4 rings in the coolant
 - Guide Tube: 4 rings inside the tube, 1 clad ring, 1 outer coolant ring
 - Azimuthal: 24 slices
 - Axial: 300 layers
 - Total: 676,800



3x3 Model: Results



Midplane Temperature Distribution

- Appropriate level of symmetry (1 symmetry line)
- Significant temperature difference between MOX and UO₂ pins.
- Pins near guide tube are warmer due to increased moderation.
- Azimuthally (as well as axially) varying heat flux around each pin.
- Power distribution shows the effect of self-shielding.